

A Fast Multigrid Algorithm for Isotropic Transport Problems I: Pure Scattering ^{*}

T. Manteuffel[†], S. McCormick[†], J. Morel[‡], S. Oliveira[§] and G. Yang[§]

Abstract

A multigrid method for solving the 1-D slab-geometry S_N equations with isotropic scattering and no absorption is presented. This scheme is highly compatible with massively parallel computer architectures and represents a first step towards similar multigrid methods for the S_N equations in curvilinear and multi-dimensional geometries. Extensive theoretical analyses are given for our scheme which indicate that it is extremely efficient. In fact, the method is so efficient that it very nearly represents an exact solution technique. Results from calculations are presented which validate the theoretical results. The case with absorption is treated in a sequel to this paper [12].

§1. Introduction

In this paper we describe a fast method for solving the equations used to model the transport of neutral particles with isotropic scattering in slab geometry. These problems are important in many applications such as nuclear reactor design, radiation therapy in medical science, radiation effects on global weather, and are a fundamental part of many algorithms used to model more complicated applications such as satellite electronics shielding. For example, a multigrid technique for the solution of highly forward-peaked anisotropic scattering in slab geometry requires the solution of an isotropic problem at the coarsest level (Morel and Manteuffel [15]). The main focus of this paper is the extensive theoretical results which we have obtained for our multigrid method. The matrix analysis techniques which we use are quite different from the Fourier analysis techniques traditionally used in numerical transport theory (e.g., see Morel and Manteuffel [15]). Since these matrix techniques yield information which is not usually available from a Fourier analysis, they represent a valuable alternative to Fourier analysis.

^{*}This work was supported by AFOSR under grant AFOSR 86-0126, the NSF under grant DMS-8704169, the DOE under grant DE-FG02-90ER25086 and Los Alamos National Laboratory.

[†]Program in Applied mathematics, University of Colorado at Boulder, Boulder, CO

[‡]Computer Research Group (C-3), Los Alamos National Laboratory, Los Alamos, NM

[§]Center for Computational Mathematics, University of Colorado of Denver, Denver, CO

The linear Boltzman equation, which is used to model neutral-particle transport, reduces to the following equation in slab geometry with isotropic scattering. The physical domain is a semi-infinite slab of width $b - a$ in the x dimension. Although three dimensional, we assume the flux of particles is independent of the y and z coordinates. Thus, the Linear Boltzman equation reduces to

$$(1.1) \quad \mu \frac{\partial \psi}{\partial x} + \sigma_t \psi = \frac{\sigma_s}{2} \int_{-1}^1 \psi(x, \mu') d\mu' + q(x, \mu),$$

for $x \in (a, b)$, $\mu \in [-1, 1]$, where $\psi(x, \mu)$ represents the flux of particles at position x traveling at an angle θ from the x -axis ($\mu = \cos(\theta)$). Here $\sigma_t dx$ represents the expected number of interactions (absorptive or scattering) that a particle will have in traveling a distance dx . In a similar manner, $\sigma_s dx$ represents the expected number of scattering interactions while $\sigma_a = \sigma_t - \sigma_s$ represents the expected number of absorptive interactions. Finally, $q(x, \mu)$ represents the particle source.

The solution is well defined if the flux of particles entering the slab is given as boundary conditions:

$$(1.2) \quad \psi(a, \mu) = g_a(\mu), \quad \psi(b, -\mu) = g_b(\mu) \quad \mu \in (0, 1).$$

The problem (1.1) becomes difficult to solve in the optically dense or thick diffusion limit. Physically, the thick limit implies that the mean-free-path between collisions that is small compared to the width of the slab. If, in addition, the material allows very little absorption, the model resembles diffusion away from boundaries and sources. Mathematically, we have

$$(1.3) \quad \sigma_t \rightarrow \infty, \quad \frac{\sigma_s}{\sigma_t} \rightarrow 1.$$

Dividing (1.1) by σ_t and taking the limits in (1.3) yields

$$(1.4) \quad \psi(x, \mu) = \frac{1}{2} \int_{-1}^1 \psi(x, \mu') d\mu',$$

which admits any $\psi(x, \mu)$ that is independent of μ . Thus, in this limit (1.1) is singularly perturbed with a large near null space. The problems near the thick diffusion limit are difficult to solve for traditional transport methods.

Numerical approximations of (1.1) suffer several difficulties in this limit. Many difference schemes yield inaccurate solutions in this limit even for well behaved solutions. For a discussion of this issue see Larsen and Morel[8]. One difference scheme that behaves well in the thick limit is the Modified Linear Discontinuous Scheme(*MLD*)([8]). Not only does it give the proper behavior in the thick limit but it is very accurate. The algorithm described in this paper will address the solution of the transport equation with S_N discretization in angle (See Section 2) using *MLD* in space.

Even when the difference scheme behaves properly in the thick limit it may be difficult to solve the resulting discrete equations. The Diffusion Synthetic Acceleration(*DSA*)

scheme was developed to address this difficulty(Alcouffe[2]). *DSA* is based upon the recognition that in the thick limit the transport of particles becomes diffusive in nature. The flux is nearly independent of direction except near the boundaries and sources. *DSA* involves solving a diffusion equation as a preconditioning for the transport equations (See Faber and Manteuffel[5]). In theory, it achieves a convergence factor bounded by approximately .23 per iteration independent of σ_t or the cell width h .

In this paper we present a multigrid algorithm that is much faster than *DSA* and avoids some of the problems associated with *DSA*. In general, the *DSA* algorithm requires a certain degree of consistency between the S_N spatial discretization scheme and the diffusion spatial discretization scheme. In recent work Larsen [6], Morel and Larsen [14] and Adams and Martin [1] have derived methods for finding consistent diffusion schemes. In [1] a scheme was developed in which the convergence factor goes to zero as $\sigma_t h$ gets large. However, *DSA* works because the transport model becomes diffusive in the thick limit. Such problems are usually amenable to multigrid techniques directly. Moreover, the difficulties associated with deriving and solving consistent *DSA* diffusion equations increase with higher dimensions.

The multigrid techniques described here have a natural generalization to higher dimensions and, as mentioned previously, can be used in conjunction with the multigrid algorithm for anisotropic problems described in Morel and Manteuffel[15]. While any generalization to higher dimensions is fraught with peril, we feel that the multigrid algorithm algorithms presented here can be successfully extended.

Although similar in spirit, our multigrid method is much more efficient than those of Nowak [16] [17], Nowak and Larsen [18], Barnett, Morel, and Harris [3] and Nowak, Morel and Harris [19]. These methods require an expensive relaxation and do not achieve a convergence factor that approaches zero in the thick diffusion limit.

In this paper, we concentrate on pure scattering, that is, no absorption, which is modeled by setting $\sigma_s = \sigma_t$. Convergence proofs for both the thick and thin limits are developed. The efficacy of the algorithm is demonstrated with numerical examples. The model with absorption, i. e., $\sigma_s < \sigma_t$, is addressed in a sequel to this paper, [12]. In this paper piecewise linear discontinuous elements are used for the spatial discretization. In [12] piecewise kinked-linear discontinuous elements are used in the thick cell limit. The proofs in this paper are used to develop asymptotic estimates for the algorithm in [12].

The remainder of this paper is organized as follows. In Section 2 we describe the discrete transport equation. We use an S_N approximation in direction (angle), and modified piecewise linear discontinuous elements (MLD) for the spatial discretization. In Section 3 we develop a two-cell, red/black, block μ -line relaxation. The fact that the scattering operator is rank-1 allows for a very efficient μ -line relaxation. Letting h_i be the width of cell i , we show

a) for $\max(\sigma_t h_{2i-1}, \sigma_t h_{2i}) \ll 1$ at two neighboring cells $2i-1$ and $2i$, the μ -line relaxation leaves the error linear across the two cells up to order $O(\max(\sigma_t^2 h_{2i-1}^2, \sigma_t^2 h_{2i}^2))$.

b) for $\min(\sigma_t h_{2i-1}, \sigma_t h_{2i}) \gg 1$, the μ -line relaxation leaves the error linear across the two cells up to order $O(\max(\frac{1}{\sigma_t h_{2i-1}}, \frac{1}{\sigma_t h_{2i}}))$.

In Section 4 we combine the relaxation with a multigrid algorithm and derive two-grid convergence rates, ρ ;

a) for $\max_i (\sigma_t h_i) \ll 1$, $\rho = O(\max_i (\sigma_t h_i)^2)$,

b) for $\min_i (\sigma_t h_i) \gg 1$, $\rho = O(\max_i (\frac{1}{\sigma_t h_i}))$.

In Section 5.1 we present numerical results for our multigrid method for both uniform and highly nonuniform grids. They yield the following convergence factor, ρ , for a V(1,1) cycle:

a) for $\max_i (\sigma_t h_i) \ll 1$, $\rho = O(\max_i (\sigma_t h_i)^3)$,

b) for $\min_i (\sigma_t h_i) \gg 1$, $\rho = O(\frac{1}{\min_i (\sigma_t h_i)^2})$,

with a slowest rate of $\rho \sim 0.01$ occurring for $\sigma_t h \sim 0.01$. These rates make a single V(1,1) cycle nearly an exact solver, especially in the thick and thin limits. The cost of a V(1,1) cycle is on the same order as 4 sweeps across the computational grid. This represents a significant savings over DSA. Moreover, the algorithm was designed to be highly parallel. We have implemented the algorithm on the Thinking Machines Inc., CM-2 at Los Alamos National Labs. These results appear in (Manteuffel et.al, [10], [11]). In Section 5.2 we present numerical results for a DSA scheme for the MLD equations. Section 6 contains concluding remarks.

§2. The Discrete Model

The angle dependence in (1.1) is discretized by a S_N approximation (c.f. Lewis and Miller [9]), that is, we assume

$$(2.1) \quad \psi(x, \mu) = \sum_{l=0}^{N-1} (2l+1) \phi_l(x) p_l(\mu),$$

where $p_l(\mu)$ is the l^{th} Legendre polynomial and $(2l+1)$ is a normalization factor. If standard Galerkin formulation is used, a system of equations, for the $\phi_l(x)$'s, called the moment equations, is established. The moments may be found by

$$(2.2) \quad \phi(x) = \frac{1}{2} \int_{-1}^1 \psi_l(x, \mu') p_l(\mu') d\mu' = \sum_{k=1}^N \omega_k \psi_l(x, \mu_k) p_l(\mu_k) d\mu',$$

where $\omega_1, \dots, \omega_N$ and μ_1, \dots, μ_N are the Gauss quadrature weights and points respectively. The second equality is exact because of the assumption (2.1). Thus, finding $\psi_j(x) = \psi(x, \mu_j)$ for $j=1, \dots, N$ is equivalent to finding the moments. A simple transformation

of the moment equations yields a system for the $\psi_j(x)$'s, called the flux equations, as follows

$$(2.3) \quad \mu_j \frac{\partial \psi_j(x)}{\partial x} + \sigma_t \psi_j(x) = \sigma_s \sum_{k=1}^N \omega_k \psi_k(x) + q_j(x),$$

for $j=1, \dots, N$.

For our purposes here we choose to differentiate the positive and negative direction. Assume N is even and let $n = N/2$, the Gauss quadrature points are symmetric about the origin and can be denoted as $-\mu_n < \dots < -\mu_1 < 0 < \mu_1 < \dots, \mu_n$. Likewise, the weight associated with $-\mu_j$ will equal the weight associated with μ_j . We define

$$(2.4a) \quad \psi_j^+(x) = \psi(x, \mu_j),$$

$$(2.4b) \quad \psi_j^-(x) = \psi(x, -\mu_j),$$

for $j = 1, \dots, n$. Equation(2.3) becomes the pair of equations

$$(2.5a) \quad \mu_j \frac{\partial \psi_j^+(x)}{\partial x} + \sigma_t \psi_j^+(x) = \sigma_s \sum_{k=1}^n \omega_k (\psi_k^+(x) + \psi_k^-(x)) + q_j^+(x),$$

$$(2.5b) \quad \mu_j \frac{\partial \psi_j^-(x)}{\partial x} + \sigma_t \psi_j^-(x) = \sigma_s \sum_{k=1}^n \omega_k (\psi_k^+(x) + \psi_k^-(x)) + q_j^-(x),$$

for $j = 1, \dots, n$. The boundary conditions (1.2) become

$$(2.6a) \quad \psi_j^+(a) = g_a(\mu_j),$$

$$(2.6b) \quad \psi_j^-(b) = g_b(\mu_j),$$

for $j = 1, \dots, n$.

The space dependence is now discretized by the Modified Linear Discontinuous difference scheme (Larsen and Morel[8]). The *MLD* scheme can be derived by using finite element methods. We first describe the Linear Discontinuous difference scheme (LD)[8]. Consider a set of grid points given by

$$(2.7) \quad a = x_{\frac{1}{2}} < x_{\frac{3}{2}} < \dots < x_{m+\frac{1}{2}} = b.$$

These represent cell edges. The centers are given by

$$(2.8) \quad x_i = \frac{1}{2}(x_{i-\frac{1}{2}} + x_{i+\frac{1}{2}}) \quad \text{for} \quad i = 1, \dots, m,$$

and the cell width is $h_i = x_{i+\frac{1}{2}} - x_{i-\frac{1}{2}}$ and m is the number of cells. We start by forming piecewise linear trial spaces. However, a different space is used for $\psi_j^+(x)$ than for $\psi_j^-(x)$. For $\psi_j^+(x)$ (for each j), we choose break points at

$$(2.9a) \quad x_{\frac{1}{2}} < \hat{x}_1^+ < x_{\frac{3}{2}} < \dots < x_{i-\frac{1}{2}} < \hat{x}_i^+ < x_{i+\frac{1}{2}} < \dots$$

with $\hat{x}_i^+ = x_{i-\frac{1}{2}} + \epsilon_i$, while for $\psi_j^-(x)$ (for each j) we choose break points at

$$(2.9b) \quad x_{\frac{1}{2}} < \hat{x}_1^- < x_{\frac{3}{2}} < \dots < x_{i-\frac{1}{2}} < \hat{x}_i^- < x_{i+\frac{1}{2}} < \dots$$

with $\hat{x}_i^- = x_{i+\frac{1}{2}} - \epsilon_i$. Here ϵ_i is small. Bases elements for the two spaces, which we denote as $V_{h,\epsilon}^+$ and $V_{h,\epsilon}^-$, are depicted in Figures 1 and 2 respectively.

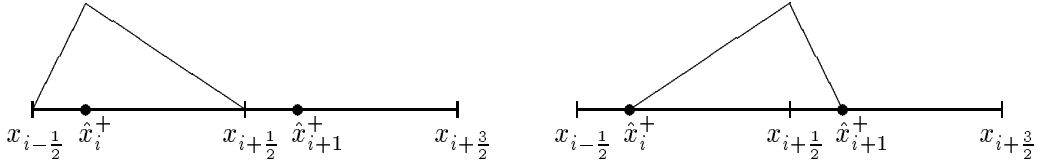


Figure 1

Bases for $V_{h,\epsilon}^+$

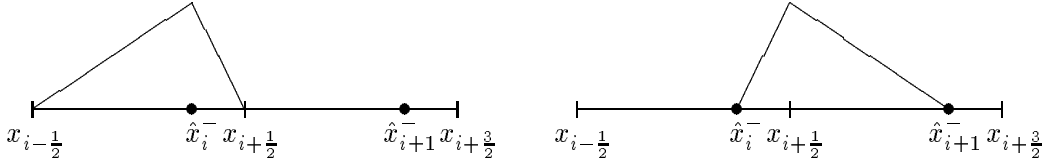


Figure 2

Bases for $V_{h,\epsilon}^-$

We assume that $\psi_j^+(x)$ and $\psi_j^-(x)$ can be expressed as a linear combination of the bases elements in $V_{h,\epsilon}^+$ and $V_{h,\epsilon}^-$ respectively. We denote

$$(2.10a) \quad \psi_{i+\frac{1}{2},j}^+ = \psi_j^+(x_{i+\frac{1}{2}}), \quad \psi_{i+\frac{1}{2},j}^- = \psi_j^-(x_{i+\frac{1}{2}}),$$

$$(2.10b) \quad \hat{\psi}_{i,j}^+ = \psi_j^+(\hat{x}_i^+), \quad \hat{\psi}_{i,j}^- = \psi_j^-(\hat{x}_i^-),$$

We also denote

$$(2.10c) \quad \psi_{i,j}^+ = \psi_j^+(x_i), \quad \psi_{i,j}^- = \psi_j^-(x_i),$$

It is important to note that $\hat{\psi}_{i,j}^+$ and $\hat{\psi}_{i,j}^-$ can be expressed in terms of values of $\psi_j^+(x)$ and $\psi_j^-(x)$ at the cell edges and cell center. Since $\psi_j^+(x)$ and $\psi_j^-(x)$ are assumed to be linear, $\hat{\psi}_{i,j}^+$ and $\hat{\psi}_{i,j}^-$ can be found as an extrapolation from the center and edge. We have

$$(2.11a) \quad \hat{\psi}_{i,j}^+ = 2\left(\frac{h_i - \epsilon_i}{h_i}\right)\psi_{i,j}^+ - \left(\frac{h_i - 2\epsilon_i}{h_i}\right)\psi_{i+\frac{1}{2},j}^+,$$

$$(2.11b) \quad \hat{\psi}_{i,j}^- = 2\left(\frac{h_i - \epsilon_i}{h_i}\right)\psi_{i,j}^- - \left(\frac{h_i - 2\epsilon_i}{h_i}\right)\psi_{i-\frac{1}{2},j}^-.$$

The Linear Discontinuous (LD) difference Scheme is derived by applying a standard Galerkin Formulation, then taking the limit as $\max_i(\epsilon_i) \rightarrow 0$. One way to construct the equations is to plug the trial space representation into (2.5a) and (2.5b) and integrate over each cell against the constant function and then against the linear function, $(x - x_i)$. This will yield a set of equations involving ϵ_i . The final equations are found by setting $\epsilon_i = 0$.

The Modified Linear Discontinuous Scheme (MLD) is found in a similar manner. As in the LD scheme, (2.5a) and (2.5b) are integrated over each cell against the constant function. Then after setting $\epsilon_i = 0$ we get the following equations

$$(2.12a) \quad \mu_j(\psi_{i+\frac{1}{2},j}^+ - \psi_{i-\frac{1}{2},j}^+) + \sigma_t \left(\frac{\hat{\psi}_{i,j}^+ + \psi_{i+\frac{1}{2},j}^+}{2}\right)h_i = \sigma_s \sum_{k=1}^n \omega_k (\hat{\psi}_{i,k}^+ + \psi_{i+\frac{1}{2},k}^+ + \hat{\psi}_{i,k}^- + \psi_{i-\frac{1}{2},k}^-)h_i + q_{i,j}^+ h_i,$$

$$(2.12b) \quad \mu_j(\psi_{i+\frac{1}{2},j}^- - \psi_{i-\frac{1}{2},j}^-) + \sigma_t \left(\frac{\hat{\psi}_{i,j}^- + \psi_{i-\frac{1}{2},j}^-}{2}\right)h_i = \sigma_s \sum_{k=1}^n \omega_k (\hat{\psi}_{i,k}^- + \psi_{i+\frac{1}{2},k}^- + \hat{\psi}_{i,k}^+ + \psi_{i-\frac{1}{2},k}^+)h_i + q_{i,j}^- h_i.$$

These are referred to as the balance equations. Instead of integration against linear functions, as in *LD*, now the equations (2.5a) are collocated at \hat{x}_i^- , equations (2.5b) are collocated at \hat{x}_i^+ , and the limit is taken as $\max_i \epsilon_i \rightarrow 0$. This yields the following equations referred to as edge equations.

$$(2.13a) \quad \mu_j \left(\frac{\psi_{i+\frac{1}{2},j}^+ - \hat{\psi}_{i,j}^+}{h_i}\right) + \sigma_t \psi_{i+\frac{1}{2},j}^+ = \sigma_s \sum_{k=1}^n \omega_k (\psi_{i+\frac{1}{2},k}^+ + \hat{\psi}_{i,k}^-) + q_{i+\frac{1}{2},j}^+,$$

$$(2.13b) \quad \mu_j \left(\frac{\hat{\psi}_{i,j}^- - \psi_{i-\frac{1}{2},j}^-}{h_i}\right) + \sigma_t \psi_{i-\frac{1}{2},j}^- = \sigma_s \sum_{k=1}^n \omega_k (\hat{\psi}_{i,k}^+ + \psi_{i-\frac{1}{2},k}^-) + q_{i-\frac{1}{2},j}^-.$$

This may be formalized as integration of (2.5a) against $\delta(x - \hat{x}_i^-)$ and (2.5b) against $\delta(x - \hat{x}_i^+)$. Note from (2.11a, b) that we may replace $\hat{\psi}_{i,k}^+$ and $\hat{\psi}_{i,k}^-$ with $2\psi_{i,k}^+ - \psi_{i+\frac{1}{2},k}^+$ and

Since B_i is diagonal, this is a trivial operation. Likewise, the negative angles could be found in a backward sweep.

This process represents x -line relaxation (also known as a source iteration or transport sweep). If we reorder the unknowns by cells and examine the effect of a complete x -line relaxation, the resulting error equation for a single cell can be written as

$$(3.3) \quad \begin{bmatrix} I + 2B_i & 0 & -2B_i & 0 \\ 0 & I & 0 & -B_i \\ -B_i & 0 & I & 0 \\ 0 & -2B_i & 0 & I + 2B_i \end{bmatrix} \begin{bmatrix} \underline{e}_{i-\frac{1}{2}}^- \\ \underline{e}_i^+ \\ \underline{e}_i^- \\ \underline{e}_{i+\frac{1}{2}}^+ \end{bmatrix}^{l+1} = \begin{bmatrix} R & 2R & 0 & -R \\ 0 & R & R & 0 \\ 0 & R & R & 0 \\ -R & 0 & 2R & R \end{bmatrix} \begin{bmatrix} \underline{e}_{i-\frac{1}{2}}^- \\ \underline{e}_i^+ \\ \underline{e}_i^- \\ \underline{e}_{i+\frac{1}{2}}^+ \end{bmatrix}^l + \begin{bmatrix} 0 \\ B_i \underline{e}_{i-\frac{1}{2}}^+ \\ B_i \underline{e}_{i+\frac{1}{2}}^- \\ 0 \end{bmatrix}^{l+1}.$$

Here l is the relaxation step. When $\sigma_i h_i \gg 1$, x -line relaxation is not effective. Equation (2.16a) reveals that, when $\sigma_i h_i \rightarrow \infty$, B_i approaches zero. Then, an x -line relaxation nearly reproduces the component of the error that is independent of angle. Since this does not affect any spatial frequency, the resulting error is not smooth in space. Any error that is independent of angle will not be suppressed regardless of its spatial frequency. This makes x -line relaxation inappropriate for use in a multigrid scheme, since even if $\sigma_i h_i$ is small on the finest grid, it will become large on coarser grids.

On the other hand, we can rearrange equation (2.17) to reveal the form of two-cell red-black block μ -line relaxations. By two-cell red-black block μ -line relaxation, we mean that at cells i and $i + 1$, we set $\underline{\psi}_{i-\frac{1}{2}}^+$ and $\underline{\psi}_{i+\frac{3}{2}}^-$ as boundary values and solve all other interior values in cells i and $i + 1$ simultaneously. This relaxation is carried out in a red-black ordering. Since the relaxation uses a red-black ordering, we can look at each 2-cell pair individually. For 2-cell pair i and $i + 1$, the errors at these two cells after the relaxation will be

$$(3.4) \quad \begin{bmatrix} \underline{e}_{i-\frac{1}{2}}^- \\ \underline{e}_i^+ \\ \underline{e}_i^- \\ \underline{e}_{i+\frac{1}{2}}^+ \\ \underline{e}_{i+\frac{1}{2}}^- \\ \underline{e}_{i+1}^+ \\ \underline{e}_{i+1}^- \\ \underline{e}_{i+\frac{3}{2}}^+ \end{bmatrix} = \begin{bmatrix} A_i & -C_i \\ -D_{i+1} & A_{i+1} \end{bmatrix}^{-1} \begin{bmatrix} 0 \\ B_i \underline{e}_{i-\frac{1}{2}}^+ \\ 0 \\ 0 \\ 0 \\ 0 \\ B_{i+1} \underline{e}_{i+\frac{3}{2}}^- \\ 0 \end{bmatrix}.$$

The inversion of the $\begin{bmatrix} A_i & -C_i \\ -D_{i+1} & A_{i+1} \end{bmatrix}$ is inexpensive since R is rank one and I , B_i , and

$$(3.9b) \quad a_{33} = a_{44} = \sum_{j=1}^n \frac{2\omega_j(\mu_j + 2\frac{\mu_j^2}{\sigma_t h_{i+1}})}{\sigma_t h_{i+1}(1 + 2\frac{\mu_j}{\sigma_t h_{i+1}} + 2\frac{\mu_j^2}{\sigma_t^2 h_{i+1}^2})},$$

$$(3.9c) \quad a_{13} = - \sum_{j=1}^n \frac{2\omega_j(\frac{\mu_i^2}{\sigma_t^2 h_i^2} + \frac{\mu_j^3}{\sigma_t^3 h_i^2 h_{i+1}})}{(1 + 2\frac{\mu_j}{\sigma_t h_i} + 2\frac{\mu_j^2}{\sigma_t^2 h_i^2})(1 + 2\frac{\mu_j}{\sigma_t h_{i+1}} + 2\frac{\mu_j^2}{\sigma_t^2 h_{i+1}^2})},$$

$$(3.9d) \quad a_{14} = - \sum_{j=1}^n \frac{2\omega_j \mu_i^3}{\sigma_t^3 h_i^2 h_{i+1}(1 + 2\frac{\mu_j}{\sigma_t h_i} + 2\frac{\mu_j^2}{\sigma_t^2 h_i^2})(1 + 2\frac{\mu_j}{\sigma_t h_{i+1}} + 2\frac{\mu_j^2}{\sigma_t^2 h_{i+1}^2})},$$

$$(3.9e) \quad a_{23} = - \sum_{j=1}^n \frac{2\omega_j(\frac{\mu_j}{\sigma_t h_i} + \frac{\mu_j^2}{\sigma_t^2 h_i^2} + \frac{\mu_j^2(1 + \frac{\mu_j}{\sigma_t h_i})}{\sigma_t^2 h_i h_{i+1}})}{(1 + 2\frac{\mu_j}{\sigma_t h_i} + 2\frac{\mu_j^2}{\sigma_t^2 h_i^2})(1 + 2\frac{\mu_j}{\sigma_t h_{i+1}} + 2\frac{\mu_j^2}{\sigma_t^2 h_{i+1}^2})},$$

$$(3.9f) \quad a_{24} = - \sum_{j=1}^n \frac{2\omega_j \frac{\mu_j^2}{\sigma_t^2 h_i h_{i+1}}(1 + \frac{\mu_j}{\sigma_t h_i})}{(1 + 2\frac{\mu_j}{\sigma_t h_i} + 2\frac{\mu_j^2}{\sigma_t^2 h_i^2})(1 + 2\frac{\mu_j}{\sigma_t h_{i+1}} + 2\frac{\mu_j^2}{\sigma_t^2 h_{i+1}^2})},$$

$$(3.9g) \quad a_{31} = - \sum_{j=1}^n \frac{2\omega_j \frac{\mu_j^2}{\sigma_t^2 h_i h_{i+1}}(1 + \frac{\mu_j}{\sigma_t h_{i+1}})}{(1 + 2\frac{\mu_j}{\sigma_t h_i} + 2\frac{\mu_j^2}{\sigma_t^2 h_i^2})(1 + 2\frac{\mu_j}{\sigma_t h_{i+1}} + 2\frac{\mu_j^2}{\sigma_t^2 h_{i+1}^2})},$$

$$(3.9h) \quad a_{32} = - \sum_{j=1}^n \frac{2\omega_j(\frac{\mu_j}{\sigma_t h_{i+1}} + \frac{\mu_j^2}{\sigma_t^2 h_{i+1}^2} + \frac{\mu_j^2(1 + \frac{\mu_j}{\sigma_t h_{i+1}})}{\sigma_t^2 h_i h_{i+1}})}{(1 + 2\frac{\mu_j}{\sigma_t h_i} + 2\frac{\mu_j^2}{\sigma_t^2 h_i^2})(1 + 2\frac{\mu_j}{\sigma_t h_{i+1}} + 2\frac{\mu_j^2}{\sigma_t^2 h_{i+1}^2})},$$

$$(3.9i) \quad a_{41} = - \sum_{j=1}^n \frac{2\omega_j \mu_i^3}{\sigma_t^3 h_i h_{i+1}^2(1 + 2\frac{\mu_j}{\sigma_t h_i} + 2\frac{\mu_j^2}{\sigma_t^2 h_i^2})(1 + 2\frac{\mu_j}{\sigma_t h_{i+1}} + 2\frac{\mu_j^2}{\sigma_t^2 h_{i+1}^2})},$$

$$(3.9j) \quad a_{42} = - \sum_{j=1}^n \frac{2\omega_j(\frac{\mu_i^2}{\sigma_t^2 h_{i+1}^2} + \frac{\mu_j^3}{\sigma_t^3 h_i h_{i+1}^2})}{(1 + 2\frac{\mu_j}{\sigma_t h_i} + 2\frac{\mu_j^2}{\sigma_t^2 h_i^2})(1 + 2\frac{\mu_j}{\sigma_t h_{i+1}} + 2\frac{\mu_j^2}{\sigma_t^2 h_{i+1}^2})},$$

Since $(I - W^T A_0^{-1} V)$ is a 4 by 4 matrix, its inversion can be obtained inexpensively and explicitly by a direct method. It is obvious that no matter how many moments are used in (2.1), the μ -line relaxation can be carried out with the same insignificant expense.

The next three theorems examine the properties of two-cell red-black block μ -line relaxation. In the first theorem we consider the S_2 problem, that is, one positive and one negative μ . We assume the number of cells m is an even number.

Theorem 1 *For S_2 , the errors after two-cell red-black μ -line relaxation will be piecewise linear across two cells.*

Proof: Since we use red-black relaxation, we can just examine each pair of two cells individually. When there is only one angle in the positive direction and one in the negative direction, $R = \frac{1}{2}, B_k = \frac{\mu_1}{\sigma_t h_k}, k = 1, \dots, m$. At cells $2i - 1$ and $2i$, after a relaxation, the error equation (3.4) becomes

$$(3.10) \quad \begin{bmatrix} \underline{e}_{2i-\frac{3}{2}}^- \\ \underline{e}_{2i-1}^+ \\ \underline{e}_{2i-1}^- \\ \underline{e}_{2i-\frac{1}{2}}^+ \\ \underline{e}_{2i-\frac{1}{2}}^- \\ \underline{e}_{2i}^+ \\ \underline{e}_{2i}^- \\ \underline{e}_{2i+\frac{1}{2}}^+ \end{bmatrix} = \begin{bmatrix} A_{2i-1} & -C_{2i-1} \\ -D_{2i} & A_{2i} \end{bmatrix}^{-1} \begin{bmatrix} 0 \\ B_{2i-1} \underline{e}_{2i-\frac{3}{2}}^+ \\ 0 \\ 0 \\ 0 \\ 0 \\ B_{2i} \underline{e}_{2i+\frac{1}{2}}^- \\ 0 \end{bmatrix}.$$

By setting $n = 1$, the explicit form of $\begin{bmatrix} A_{2i-1} & -C_{2i-1} \\ -D_{2i} & A_{2i} \end{bmatrix}^{-1}$ can be easily obtained by Sherman-Morrison formula (3.7). After multiplication in (3.10), we have

$$(3.11) \quad \begin{bmatrix} \underline{e}_{2i-\frac{3}{2}}^- \\ \underline{e}_{2i-1}^+ \\ \underline{e}_{2i-1}^- \\ \underline{e}_{2i-\frac{1}{2}}^+ \\ \underline{e}_{2i-\frac{1}{2}}^- \\ \underline{e}_{2i}^+ \\ \underline{e}_{2i}^- \\ \underline{e}_{2i+\frac{1}{2}}^+ \end{bmatrix} = \frac{\sigma_t h_{2i}}{2\mu_1 + \sigma_t h_{2i-1} + \sigma_t h_{2i}} \begin{bmatrix} 1 + \frac{h_{2i-1}}{h_{2i}} \\ 1 + \frac{h_{2i-1}}{2h_{2i}} + \frac{2\mu_1}{\sigma_t h_{2i}} \\ 1 + \frac{h_{2i-1}}{2h_{2i}} \\ 1 + \frac{2\mu_1}{\sigma_t h_{2i}} \\ 1 \\ \frac{1}{2} + \frac{2\mu_1}{\sigma_t h_{2i}} \\ \frac{1}{2} \\ \frac{2\mu_1}{\sigma_t h_{2i}} \end{bmatrix} \underline{e}_{2i-\frac{3}{2}}^+$$

$$+ \frac{\sigma_t h_{2i-1}}{2\mu_1 + \sigma_t h_{2i-1} + \sigma_t h_{2i}} \begin{bmatrix} \frac{2\mu_1}{\sigma_t h_{2i-1}} \\ \frac{1}{2} \\ \frac{1}{2} + \frac{2\mu_1}{\sigma_t h_{2i-1}} \\ 1 \\ 1 + \frac{2\mu_1}{\sigma_t h_{2i-1}} \\ 1 + \frac{h_{2i}}{2h_{2i-1}} \\ 1 + \frac{h_{2i}}{2h_{2i-1}} + \frac{2\mu_1}{\sigma_t h_{2i-1}} \\ 1 + \frac{h_{2i}}{h_{2i-1}} \end{bmatrix} e_{2i+\frac{1}{2}}^-.$$

The errors fit the following linear formulas:

$$(3.12a) \quad e_k^- = \frac{\sigma_t h_{2i}}{2\mu_1 + \sigma_t h_{2i-1} + \sigma_t h_{2i}} \left(1 + \frac{h_{2i-1}}{h_{2i}} - \frac{\xi_k}{h_{2i}}\right) e_{2i-\frac{3}{2}}^+ + \frac{\sigma_t h_{2i-1}}{2\mu_1 + \sigma_t h_{2i-1} + \sigma_t h_{2i}} \left(\frac{2\mu_1}{\sigma_t h_{2i-1}} + \frac{\xi_k}{h_{2i-1}}\right) e_{2i+\frac{1}{2}}^-,$$

where $k = 2i - \frac{3}{2}, 2i - 1, 2i - \frac{1}{2}, 2i$, and $\xi_k = 0, \frac{h_{2i-1}}{2}, h_{2i-1}, h_{2i-1} + \frac{h_{2i}}{2}$ correspondingly and

$$(3.12b) \quad e_k^+ = \frac{\sigma_t h_{2i}}{2\mu_1 + \sigma_t h_{2i-1} + \sigma_t h_{2i}} \left(1 + \frac{h_{2i-1}}{h_{2i}} + \frac{2\mu_1}{\sigma_t h_{2i}} - \frac{\xi_k}{h_{2i}}\right) e_{2i-\frac{3}{2}}^+ + \frac{\sigma_t h_{2i-1} \xi_k}{h_{2i-1} (2\mu_1 + \sigma_t h_{2i-1} + \sigma_t h_{2i})} e_{2i+\frac{1}{2}}^-,$$

where $k = 2i - 1, 2i - \frac{1}{2}, 2i, 2i + \frac{1}{2}$, and $\xi_k = \frac{h_{2i-1}}{2}, h_{2i-1}, h_{2i-1} + \frac{h_{2i}}{2}, h_{2i-1} + h_{2i}$ correspondingly. Since after relaxation the errors fit linear formulas at both the positive and negative angle direction, the errors are linearly distributed across two cells. \square

Let us define a new cell i on a coarser grid \hat{h} whose length \hat{h}_i is $\hat{h}_i = h_{2i-1} + h_{2i}$ and it covers cells $2i - 1$ and cell $2i$. We can find values at the cell center and the edges of cell i of grid \hat{h} by letting $\xi_k = 0, \xi_k = \frac{h_{2i-1} + h_{2i}}{2}$ and $\xi_k = h_{2i-1} + h_{2i}$ in (3.12). Thus, we have

$$(3.13a) \quad e_{i-\frac{1}{2}}^{-(\hat{h})} = \frac{\sigma_t h_{2i}}{2\mu_1 + \sigma_t h_{2i-1} + \sigma_t h_{2i}} \left(1 + \frac{h_{2i-1}}{h_{2i}}\right) e_{2i-\frac{3}{2}}^+ + \frac{h_{2i-1}}{h_{2i-1} (2\mu_1 + \sigma_t h_{2i-1} + \sigma_t h_{2i})} e_{2i+\frac{1}{2}}^-,$$

$$(3.13b) \quad e_i^{+(\hat{h})} = \frac{\sigma_t h_{2i}}{2\mu_1 + \sigma_t h_{2i-1} + \sigma_t h_{2i}} \left(\frac{1}{2} + \frac{h_{2i-1}}{2h_{2i}} + \frac{2\mu_1}{\sigma_t h_{2i}}\right) e_{2i-\frac{3}{2}}^+ + \frac{\sigma_t h_{2i-1}}{2\mu_1 + \sigma_t h_{2i-1} + \sigma_t h_{2i}} \left(\frac{1}{2} + \frac{h_{2i}}{2h_{2i-1}}\right) e_{2i+\frac{1}{2}}^-,$$

$$(3.13c) \quad e_i^{-(\hat{h})} = \frac{\sigma_t h_{2i}}{2\mu_1 + \sigma_t h_{2i-1} + \sigma_t h_{2i}} \left(\frac{1}{2} + \frac{h_{2i-1}}{2h_{2i}}\right) e_{2i-\frac{3}{2}}^+ + \frac{\sigma_t h_{2i-1}}{2\mu_1 + \sigma_t h_{2i-1} + \sigma_t h_{2i}} \left(\frac{1}{2} + \frac{h_{2i}}{2h_{2i-1}} + \frac{2\mu_1}{\sigma_t h_{2i-1}}\right) e_{2i+\frac{1}{2}}^-,$$

$$(3.13d) \quad e_{i+\frac{1}{2}}^{+(\hat{h})} = \frac{\sigma_t h_{2i}}{2\mu_1 + \sigma_t h_{2i-1} + \sigma_t h_{2i}} \frac{2\mu_1}{\sigma_t h_{2i}} e_{2i-\frac{3}{2}}^+ + \frac{\sigma_t h_{2i-1}}{2\mu_1 + \sigma_t h_{2i-1} + \sigma_t h_{2i}} \left(1 + \frac{h_{2i}}{h_{2i-1}}\right) e_{2i+\frac{1}{2}}^-,$$

$$(3.20b) \quad H_1 = \begin{bmatrix} I - R & -2R & 0 & R & 0 & 0 & 0 & 0 \\ 0 & I - R & -R & 0 & 0 & 0 & 0 & 0 \\ 0 & -R & I - R & 0 & 0 & 0 & 0 & 0 \\ R & 0 & -2R & I - R & 0 & 0 & 0 & 0 \\ 0 & 0 & 0 & 0 & I - R & -2R & 0 & R \\ 0 & 0 & 0 & 0 & 0 & I - R & -R & 0 \\ 0 & 0 & 0 & 0 & 0 & -R & I - R & 0 \\ 0 & 0 & 0 & 0 & R & 0 & -2R & I - R \end{bmatrix},$$

and

$$(3.20c) \quad M = \sigma_t h_i B_i = \begin{bmatrix} \mu_1 & \cdots & 0 \\ \vdots & \ddots & \vdots \\ 0 & \cdots & \mu_n \end{bmatrix}.$$

Then

$$(3.21) \quad \begin{bmatrix} A_{2i-1} & -C_{2i-1} \\ -D_{2i} & A_{2i} \end{bmatrix}^{-1} = (I + H_0^{-1} H_1)^{-1} H_0^{-1}.$$

It is trivial to obtain

$$(3.22) \quad H_0^{-1} = \begin{bmatrix} 0 & 0 & \sigma_t h_{2i-1} M^{-1} & 0 & 0 & 0 & \sigma_t h_{2i} M^{-1} & 0 \\ 0 & \sigma_t h_{2i-1} M^{-1} & 0 & -\frac{\sigma_t h_{2i-1}}{2} M^{-1} & 0 & 0 & 0 & 0 \\ -\frac{\sigma_t h_{2i-1}}{2} M^{-1} & 0 & \sigma_t h_{2i-1} M^{-1} & 0 & 0 & 0 & \sigma_t h_{2i} M^{-1} & 0 \\ 0 & \sigma_t h_{2i-1} M^{-1} & 0 & 0 & 0 & 0 & 0 & 0 \\ 0 & 0 & 0 & 0 & 0 & 0 & \sigma_t h_{2i} M^{-1} & 0 \\ 0 & \sigma_t h_{2i-1} M^{-1} & 0 & 0 & 0 & \sigma_t h_{2i} M^{-1} & 0 & -\frac{\sigma_t h_{2i}}{2} M^{-1} \\ 0 & 0 & 0 & 0 & -\frac{\sigma_t h_{2i}}{2} M^{-1} & 0 & \sigma_t h_{2i} M^{-1} & 0 \\ 0 & \sigma_t h_{2i-1} M^{-1} & 0 & 0 & 0 & \sigma_t h_{2i} M^{-1} & 0 & 0 \end{bmatrix}.$$

When $\sigma_t h_{2i-1}, \sigma_t h_{2i} \ll 1$, $\|H_0^{-1}\| \ll 1$. Since H_1 is a constant matrix, $\|H_0^{-1} H_1\| \ll 1$. So $I + H_0^{-1} H_1$ is invertable and

$$(3.23) \quad (I + H_0^{-1} H_1)^{-1} = I - H_0^{-1} H_1 + O(\max(\sigma_t^2 h_{2i-1}^2, \sigma_t^2 h_{2i}^2)).$$

Substituting (3.23) into (3.21), we have

$$(3.24) \quad \begin{bmatrix} A_{2i-1} & -C_{2i-1} \\ -D_{2i} & A_{2i} \end{bmatrix}^{-1} = H_0^{-1} - H_0^{-1} H_1 H_0^{-1} + O(\max(\sigma_t^3 h_{2i-1}^3, \sigma_t^3 h_{2i}^3)).$$

When we carry out the arithmetic in (3.24) by using (3.20b) and (3.22) and substitute the

resulting formula into (3.10), we have the errors after relaxation as

$$(3.25) \quad \begin{bmatrix} \underline{e}_{2i-\frac{3}{2}}^- \\ \underline{e}_{2i-1}^+ \\ \underline{e}_{2i-1}^- \\ \underline{e}_{2i-\frac{1}{2}}^+ \\ \underline{e}_{2i-\frac{1}{2}}^- \\ \underline{e}_{2i}^+ \\ \underline{e}_{2i}^- \\ \underline{e}_{2i+\frac{1}{2}}^+ \end{bmatrix} = \begin{bmatrix} I \\ 0 \\ I \\ 0 \\ I \\ 0 \\ I \\ 0 \end{bmatrix} \underline{e}_{2i-\frac{3}{2}}^+ + \sigma_t h_{2i-1} \begin{bmatrix} (1 + \frac{h_{2i}}{h_{2i-1}})M^{-1}(I - R) \\ -\frac{1}{2}M^{-1}R \\ (\frac{1}{2} + \frac{h_{2i}}{h_{2i-1}})M^{-1}(I - R) \\ -M^{-1}R \\ \frac{h_{2i}}{h_{2i-1}}M^{-1}(I - R) \\ -(1 + \frac{h_{2i}}{2h_{2i-1}})M^{-1}R \\ \frac{h_{2i}}{2h_{2i-1}}M^{-1}(I - R) \\ -(1 + \frac{h_{2i}}{h_{2i-1}})M^{-1}R \end{bmatrix} \underline{e}_{2i-\frac{3}{2}}^+.$$

$$+ \begin{bmatrix} 0 \\ I \\ 0 \\ I \\ 0 \\ I \\ 0 \\ I \end{bmatrix} \underline{e}_{2i+\frac{1}{2}}^- + \sigma_t h_{2i} \begin{bmatrix} -(1 + \frac{h_{2i-1}}{h_{2i}})M^{-1}R \\ \frac{h_{2i-1}}{2h_{2i}}M^{-1}(I - R) \\ -(1 + \frac{h_{2i-1}}{2h_{2i}})M^{-1}R \\ \frac{h_{2i-1}}{h_{2i}}M^{-1}(I - R) \\ -M^{-1}R \\ (\frac{1}{2} + \frac{h_{2i-1}}{h_{2i}})M^{-1}(I - R) \\ -\frac{1}{2}M^{-1}R \\ (1 + \frac{h_{2i-1}}{h_{2i}})M^{-1}(I - R) \end{bmatrix} \underline{e}_{2i+\frac{1}{2}}^- + O(\max(\sigma_t^2 h_{2i-1}^2, \sigma_t^2 h_{2i}^2))$$

When we define the same cell i on grid \hat{h} as in Theorem 1, we have

$$(3.26a) \quad \underline{e}_{i-\frac{1}{2}}^{-(\hat{h})} = (1 - \sigma_t h_{2i-1} (1 + \frac{h_{2i}}{h_{2i-1}}))M^{-1}(I - R)\underline{e}_{2i-\frac{3}{2}}^+ + \sigma_t h_{2i} (1 + \frac{h_{2i-1}}{h_{2i}})M^{-1}R\underline{e}_{2i+\frac{1}{2}}^-,$$

$$(3.26b) \quad \underline{e}_i^{+(\hat{h})} = \sigma_t h_{2i-1} (\frac{1}{2} + \frac{h_{2i}}{2h_{2i-1}})M^{-1}R\underline{e}_{2i-\frac{3}{2}}^+ + (1 - \sigma_t h_{2i} (\frac{1}{2} + \frac{h_{2i-1}}{2h_{2i}}))M^{-1}(I - R)\underline{e}_{2i+\frac{1}{2}}^-,$$

$$(3.26c) \quad \underline{e}_i^{-(\hat{h})} = (1 - \sigma_t h_{2i-1} (\frac{1}{2} + \frac{h_{2i}}{2h_{2i-1}}))M^{-1}(I - R)\underline{e}_{2i-\frac{3}{2}}^+ + \sigma_t h_{2i} (\frac{1}{2} + \frac{2h_{2i-1}}{h_{2i}})M^{-1}R\underline{e}_{2i+\frac{1}{2}}^-,$$

$$(3.26d) \quad \underline{e}_{i+\frac{1}{2}}^{+(\hat{h})} = \sigma_t h_{2i-1} (1 + \frac{h_{2i}}{h_{2i-1}})M^{-1}R\underline{e}_{2i-\frac{3}{2}}^+ + (1 - \sigma_t h_{2i} (1 + \frac{h_{2i-1}}{2h_{2i}}))M^{-1}(I - R)\underline{e}_{2i+\frac{1}{2}}^-.$$

We can write (3.25) in terms of $\underline{e}_{i-\frac{1}{2}}^{-(\hat{h})}, \underline{e}_i^{+(\hat{h})}, \underline{e}_i^{-(\hat{h})}, \underline{e}_{i+\frac{1}{2}}^{+(\hat{h})}$ as

$$(3.27) \quad \begin{bmatrix} \underline{e}_{2i-\frac{3}{2}}^- \\ \underline{e}_{2i-1}^+ \\ \underline{e}_{2i-1}^- \\ \underline{e}_{2i-\frac{1}{2}}^+ \\ \underline{e}_{2i-\frac{1}{2}}^- \\ \underline{e}_{2i}^+ \\ \underline{e}_{2i}^- \\ \underline{e}_{2i+\frac{1}{2}}^+ \end{bmatrix} = \begin{bmatrix} T_{1,2i-1} \\ T_{2,2i-1} \end{bmatrix} \begin{bmatrix} \underline{e}_i^{-(\hat{h})} \\ \underline{e}_i^{+(\hat{h})} \\ \underline{e}_i^{-(\hat{h})} \\ \underline{e}_i^{+(\hat{h})} \end{bmatrix} + O(\max(\sigma_t^2 h_{2i-1}^2, \sigma_t^2 h_{2i}^2)).$$

Thus, the errors are piecewise linear across the two cells $2i-1$ and $2i$ up to the accuracy of $O(\max(\sigma_t^2 h_{2i-1}^2, \sigma_t^2 h_{2i}^2))$. \square

We now focus our attention on the optically dense or thick limit.

Lemma 1 . Suppose $(\sigma_t h_i) \gg 1$; then, the asymptotic inversion of A_i defined by (2.18a) can be expanded as

$$(3.28) \quad A_i^{-1} = \frac{\sigma_t h_i}{2c_0} \begin{bmatrix} R & 2R & 0 & -R \\ 0 & R & R & 0 \\ 0 & R & R & 0 \\ -R & 0 & 2R & R \end{bmatrix} + I \\ + \frac{1}{2c_0} \begin{bmatrix} -2(MR + RM) & -2(MR + RM) & 2(MR + RM) & 2MR \\ (MR - RM) & 0 & -2MR & -(MR + RM) \\ -(MR + RM) & -2MR & 0 & (MR - RM) \\ 2MR & 2(MR + RM) & -2(MR + RM) & -2(MR + RM) \end{bmatrix} + O\left(\frac{1}{\sigma_t h_i}\right).$$

Proof: Write

$$(3.29) \quad A_i = \begin{bmatrix} I + 2B_i - R & -2R & -2B_i & R \\ 0 & I - R & -R & B_i \\ B_i & -R & I - R & 0 \\ R & -2B_i & -2R & I + 2B_i - R \end{bmatrix} \\ = \begin{bmatrix} I + 2B_i & 0 & -2B_i & 0 \\ 0 & I & 0 & B_i \\ B_i & 0 & I & 0 \\ 0 & -2B_i & 0 & I + 2B_i \end{bmatrix} - \begin{bmatrix} 2\underline{1} & 0 \\ \underline{1} & \underline{1} \\ \underline{1} & \underline{1} \\ 0 & 2\underline{1} \end{bmatrix} \begin{bmatrix} \frac{1}{2}\underline{w}^T & \underline{w}^T & 0 & -\frac{1}{2}\underline{w}^T \\ -\frac{1}{2}\underline{w}^T & 0 & \underline{w}^T & \frac{1}{2}\underline{w}^T \end{bmatrix},$$

where $\underline{1} = (1, 1, \dots, 1)^T$ and $\underline{w}^T = (\omega_1, \omega_2, \dots, \omega_n)$. The first term is easily inverted while the second term is a rank two matrix. If we denote this as

$$(3.30) \quad A_i = A_0 - VW^T,$$

with A_0 denoting the first term and VW^T the second. Then the Sherman-Morrison formulas yield

$$(3.31) \quad A_i^{-1} = A_0^{-1} + A_0^{-1}V(I - W^T A_0^{-1}V)^{-1}W^T A_0^{-1}.$$

A_0^{-1} is readily given by

$$(3.32) \quad A_0 = (I + 2B_i + 2B_i^2)^{-1} \begin{bmatrix} I & 0 & 2B_i & 0 \\ 0 & I + 2B_i & 0 & -B_i \\ -B_i & 0 & I + 2B_i & 0 \\ 0 & 2B_i & 0 & I \end{bmatrix}.$$

The matrix $(I - W^T A_0^{-1}V)$ is 2×2 and its inverse can be obtained as

$$(3.33) \quad (I - W^T A_0^{-1}V)^{-1} = \xi_i \begin{bmatrix} 1 & 0 \\ 0 & 1 \end{bmatrix},$$

where

$$(3.34) \quad \xi_i = \frac{1}{1 - \zeta_i}, \quad \zeta_i = \sum_{j=1}^N \left(\frac{2\omega_j(1 + \frac{\mu_j}{\sigma_t h_i})}{1 + 2\frac{\mu_j}{\sigma_t h_i} + 2(\frac{\mu_j}{\sigma_t h_i})^2} \right).$$

In the optically dense media case, we expand ξ_i as

$$(3.35) \quad \xi_i = \frac{\sigma_t h_i}{2c_0} + O\left(\frac{1}{\sigma_t h_i}\right),$$

and

$$(3.36) \quad (I + 2B_i + 2B_i^2)^{-1} = I - \frac{2}{\sigma_t h_i}M + \frac{2}{\sigma_t^2 h_i^2}M^2 + O\left(\frac{1}{\sigma_t^3 h_i^3}\right).$$

Substituting (3.32),(3.33), (3.35) and (3.36) into (3.31), we have (3.28). \square

Theorem 3 . Suppose $\min_{k=(2i-1,2i)} (\sigma_t h_k) \gg 1$; then, the errors after the two cell red-black μ -line relaxation will be piecewise linear up to the accuracy of $O(\max(\frac{1}{\sigma_t h_{2i-1}}, \frac{1}{\sigma_t h_{2i}}))$.

Proof: When $\min_{k=(2i-1,2i)} (\sigma_t h_k) \gg 1$, we need to expand $\begin{bmatrix} A_{2i-1} & -C_{2i-1} \\ -D_{2i} & A_{2i} \end{bmatrix}^{-1}$. Write

$$(3.37) \quad \begin{bmatrix} A_{2i-1} & -C_{2i-1} \\ -D_{2i} & A_{2i} \end{bmatrix} = \begin{bmatrix} A_{2i-1} & 0 \\ -D_{2i} & A_{2i} \end{bmatrix} - \begin{bmatrix} 0 & C_{2i-1} \\ 0 & 0 \end{bmatrix} = A_0 - VW^T,$$

where

$$(3.38) \quad VW^T = \begin{bmatrix} 0 & C_{2i-1} \\ 0 & 0 \end{bmatrix},$$

with $V = (0, 0, I, 0, 0, 0, 0, 0)^T$ and $W^T = (0, 0, 0, 0, B_{2i-1}, 0, 0, 0)$. Its inversion can be obtained by Sherman-Morrison formula (3.31). We first note that

$$(3.39) \quad A_0^{-1} = \begin{bmatrix} A_{2i-1}^{-1} & 0 \\ A_{2i-1}^{-1} D_{2i} A_{2i}^{-1} & A_{2i}^{-1} \end{bmatrix}.$$

We can expand A_0^{-1} by using Lemma 1. By substituting the expansion of A_0^{-1} into $(I - W^T A_0^{-1} V)$, we can then expand $(I - W^T A_0^{-1} V)^{-1}$. The explicit expansion of $\begin{bmatrix} A_{2i-1} & -C_{2i-1} \\ -D_{2i} & A_{2i} \end{bmatrix}^{-1}$ is omitted here because of its complexity. After the expansion, the error equation (3.10) at cells $2i-1$ and $2i$ after two-cell μ -line relaxation can be expanded as

$$(3.40) \quad \begin{bmatrix} \underline{e}_{2i-\frac{3}{2}}^- \\ \underline{e}_{2i-1}^+ \\ \underline{e}_{2i-1}^- \\ \underline{e}_{2i-\frac{1}{2}}^+ \\ \underline{e}_{2i-\frac{1}{2}}^- \\ \underline{e}_{2i}^+ \\ \underline{e}_{2i}^- \\ \underline{e}_{2i+\frac{1}{2}}^+ \end{bmatrix} = \begin{bmatrix} R \\ (\frac{1}{2} + \frac{h_{2i-1}}{2(h_{2i-1}+h_{2i})})R \\ (\frac{1}{2} + \frac{h_{2i-1}}{2(h_{2i-1}+h_{2i})})R \\ \frac{h_{2i-1}}{(h_{2i-1}+h_{2i})}R \\ \frac{h_{2i-1}}{(h_{2i-1}+h_{2i})}R \\ \frac{h_{2i-1}}{2(h_{2i-1}+h_{2i})}R \\ \frac{h_{2i-1}}{2(h_{2i-1}+h_{2i})}R \\ 0 \end{bmatrix} \underline{e}_{2i-\frac{3}{2}}^+ + \begin{bmatrix} 0 \\ \frac{h_{2i-1}}{2(h_{2i-1}+h_{2i})}R \\ \frac{h_{2i-1}}{2(h_{2i-1}+h_{2i})}R \\ \frac{h_{2i-1}}{(h_{2i-1}+h_{2i})}R \\ \frac{h_{2i-1}}{(h_{2i-1}+h_{2i})}R \\ (\frac{1}{2} + \frac{h_{2i-1}}{2(h_{2i-1}+h_{2i})})R \\ (\frac{1}{2} + \frac{h_{2i-1}}{2(h_{2i-1}+h_{2i})})R \\ R \end{bmatrix} \underline{e}_{2i+\frac{1}{2}}^- + O(\max(\frac{1}{\sigma_i h_{2i-1}}, \frac{1}{\sigma_i h_{2i}})).$$

As in Theorem 1 and 2 we define the same cell i on grid \hat{h} and obtain

$$(3.41a) \quad \underline{e}_{i-\frac{1}{2}}^{-(\hat{h})} = R \underline{e}_{2i-\frac{3}{2}}^+,$$

$$(3.41b) \quad \underline{e}_i^{+(\hat{h})} = \frac{1}{2} R \underline{e}_{2i-\frac{3}{2}}^+ + \frac{1}{2} R \underline{e}_{2i+\frac{1}{2}}^-,$$

$$(3.41c) \quad \underline{e}_i^{-(\hat{h})} = \frac{1}{2} R \underline{e}_{2i-\frac{3}{2}}^+ + \frac{1}{2} R \underline{e}_{2i+\frac{1}{2}}^-,$$

$$(3.41d) \quad \underline{e}_{i+\frac{1}{2}}^{+(\hat{h})} = R \underline{e}_{2i+\frac{1}{2}}^-,$$

Then (3.40) can be written as

$$(3.42) \quad \begin{bmatrix} \underline{e}_{2i-\frac{3}{2}}^- \\ \underline{e}_{2i-1}^+ \\ \underline{e}_{2i-1}^- \\ \underline{e}_{2i-\frac{1}{2}}^+ \\ \underline{e}_{2i-\frac{1}{2}}^- \\ \underline{e}_{2i}^+ \\ \underline{e}_{2i}^- \\ \underline{e}_{2i+\frac{1}{2}}^+ \end{bmatrix} = \begin{bmatrix} T_{1,2i-1} \\ T_{2,2i-1} \end{bmatrix} \begin{bmatrix} \underline{e}_{i-\frac{1}{2}}^{-(\hat{h})} \\ \underline{e}_i^{+(\hat{h})} \\ \underline{e}_i^{-(\hat{h})} \\ \underline{e}_{i+\frac{1}{2}}^{+(\hat{h})} \end{bmatrix} + O(\max(\frac{1}{\sigma_i h_{2i-1}}, \frac{1}{\sigma_i h_{2i}})).$$

§4.1 Analysis of Convergence Factors of the Multigrid Algorithm

We start our analysis with the S_2 problem.

Theorem 4 *For the S_2 angular discretization, that is, when there is only one angle in the positive direction and one angle in the negative direction, the multigrid algorithm with two-cell red-black block μ -line relaxation will be an exact solver provided the coarsest grid is solved exactly.*

Proof: Define G^h be the two-cell red-black block μ -line relaxation matrix. The errors after the relaxation will be

$$(4.8) \quad \underline{e}_1^h = G^h \underline{e}_0^h,$$

where \underline{e}_0^h and \underline{e}_1^h are errors before and after relaxation respectively. From (3.16) in Theorem 1, the errors after the relaxation can be expressed as

$$(4.9) \quad \underline{e}_1^h = G^h \underline{e}_0^h = I_{2h}^h \underline{e}^{2h},$$

where \underline{e}^{2h} is defined on a coarse grid \hat{h} with mesh size of cell i as $\hat{h}_i = h_{2i-1} + h_{2i}$ and its cell edges at the same spatial position of left edge of cell $2i - 1$ and right edge of cell $2i$ of fine grid h . The error, \underline{e}_2^h , after one step of a two-grid multigrid $V(1, 1)$ cycle can be written in matrix form as

$$(4.10) \quad \begin{aligned} \underline{e}_2^h &= G^h (G^h \underline{e}_0^h - I_{2h}^h (A^{2h})^{-1} I_h^{2h} A^h G^h \underline{e}_0^h) \\ &= G^h (\underline{e}_1^h - I_{2h}^h (A^{2h})^{-1} I_h^{2h} A^h \underline{e}_1^h). \end{aligned}$$

Substituting (4.9) into (4.10), we have

$$(4.11) \quad \underline{e}_2^h = G^h (I_{2h}^h \underline{e}^{2h} - I_{2h}^h (A^{2h})^{-1} I_h^{2h} A^h I_{2h}^h \underline{e}^{2h}).$$

Note that the coarse grid operator A^{2h} is defined by (4.3). So (4.11) becomes

$$(4.12) \quad \underline{e}_2^h = G^h (I_{2h}^h \underline{e}^{2h} - I_{2h}^h (A^{2h})^{-1} A^{2h} \underline{e}^{2h}) = 0.$$

This means that the errors will be completely eliminated by a multigrid V-cycle provided the coarse grid $2h$ is solved exactly. By induction, the coarse grid can be solved exactly if the coarsest grid solution is exact. The coarsest grid in our algorithm contains only two cells and can be exactly solved by two-cell block μ -line relaxation. \square

For S_N with $N > 2$, the multigrid algorithm will no longer be an exact solver. However, we can establish upper bounds on the convergence factors of the multigrid algorithm when

$$\max_{k=(1,\dots,m)} (\sigma_t h_k) \ll 1 \text{ and } \min_{k=(1,\dots,m)} (\sigma_t h_k) \gg 1.$$

In the next two lemmas, we present upper bounds on the norm of the inversion of the operator A^{2h} . We use the notation $\|\cdot\|_{1,\infty}$ to indicate that the bounds hold for both the L_1 norm and the L_∞ norm.

Lemma 2 When $\max(\sigma_t \hat{h}_i, \sigma_t \hat{h}_{i+1}) \ll 1$,

$$(4.13) \quad \left\| \begin{bmatrix} A_i^{2h} & -C_i^{2h} \\ -D_{i+1}^{2h} & A_{i+1}^{2h} \end{bmatrix}^{-1} \right\|_{1,\infty} \leq c_1 \max(\sigma_t \hat{h}_i, \sigma_t \hat{h}_{i+1}),$$

where \hat{h}_i and \hat{h}_{i+1} are the coarse grid cell sizes and are defined as

$$(4.14) \quad \hat{h}_i = h_{2i-1} + h_{2i}, \quad \hat{h}_{i+1} = h_{2i+1} + h_{2i+2},$$

and c_1 is a constant independent of σ_t, \hat{h}_i and \hat{h}_{i+1} .

Proof: When $\max_{k=(2i-1, \dots, 2i+2)}(\sigma_t \hat{h}_k) \ll 1$, then $\max_{k=(i, i+1)}(\sigma_t \hat{h}_k) \ll 1$. From (3.22),

we can expand $\begin{bmatrix} A_i^{2h} & -C_i^{2h} \\ -D_{i+1}^{2h} & A_{i+1}^{2h} \end{bmatrix}^{-1}$ as

$$(4.15) \quad \begin{bmatrix} A_i^{2h} & -C_i^{2h} \\ -D_{i+1}^{2h} & A_{i+1}^{2h} \end{bmatrix}^{-1} =$$

$$\begin{bmatrix} 0 & 0 & \sigma_t \hat{h}_i M^{-1} & 0 & \sigma_t \hat{h}_{i+1} M^{-1} & 0 & \sigma_t \hat{h}_{i+1} M^{-1} & 0 \\ 0 & \sigma_t \hat{h}_i M^{-1} & 0 & -\sigma_t \hat{h}_i \frac{M^{-1}}{2} & 0 & 0 & 0 & 0 \\ -\sigma_t \hat{h}_i \frac{M^{-1}}{2} & 0 & \sigma_t \hat{h}_i M^{-1} & 0 & 0 & 0 & \sigma_t \hat{h}_{i+1} M^{-1} & 0 \\ 0 & \sigma_t \hat{h}_i M^{-1} & 0 & 0 & 0 & 0 & 0 & 0 \\ 0 & 0 & 0 & 0 & 0 & 0 & \sigma_t \hat{h}_{i+1} M^{-1} & 0 \\ 0 & \sigma_t \hat{h}_i M^{-1} & 0 & 0 & 0 & \sigma_t \hat{h}_{i+1} M^{-1} & 0 & -\sigma_t \hat{h}_{i+1} \frac{M^{-1}}{2} \\ 0 & 0 & 0 & 0 & -\sigma_t \hat{h}_{i+1} \frac{M^{-1}}{2} & 0 & \sigma_t \hat{h}_{i+1} M^{-1} & 0 \\ 0 & \sigma_t \hat{h}_i M^{-1} & 0 & \sigma_t \hat{h}_i M^{-1} & 0 & \sigma_t \hat{h}_{i+1} M^{-1} & 0 & 0 \end{bmatrix}$$

$$+ O(\max(\sigma_t^2 \hat{h}_i^2, \sigma_t^2 \hat{h}_{i+1}^2)).$$

where M is defined by (3.20c). Since M is diagonal and constant, we can find constants c_1 such that

$$(4.16) \quad \left\| \begin{bmatrix} A_i^{2h} & -C_i^{2h} \\ -D_{i+1}^{2h} & A_{i+1}^{2h} \end{bmatrix}^{-1} \right\|_{1,\infty} < c_1 \max(\sigma_t \hat{h}_i, \sigma_t \hat{h}_{i+1}).$$

□

To simplify our notation, let us define

$$(4.17a) \quad H_i = \begin{bmatrix} A_i^{2h} & -C_i^{2h} \\ -D_{i+1}^{2h} & A_{i+1}^{2h} \end{bmatrix}^{-1} \begin{bmatrix} S_{2i-1,1} & S_{2i-1,2} & 0 & 0 \\ 0 & 0 & S_{2i+1,1} & S_{2i+1,2} \end{bmatrix} \begin{bmatrix} A_{2i-1}^h & -C_{2i-1}^h & 0 & 0 \\ -D_{2i}^h & A_{2i}^h & -C_{2i}^h & 0 \\ 0 & -D_{2i+1}^h & A_{2i+1}^h & -C_{2i+1}^h \\ 0 & 0 & -D_{2i+2}^h & A_{2i+2}^h \end{bmatrix},$$

$$(4.17b) \quad U_{i+1} = \begin{bmatrix} A_i^{2h} & -C_i^{2h} \\ -D_{i+1}^{2h} & A_{i+1}^{2h} \end{bmatrix}^{-1} \begin{bmatrix} S_{2i-1,1} & S_{2i-1,2} & 0 & 0 \\ 0 & 0 & S_{2i+1,1} & S_{2i+1,2} \end{bmatrix} \begin{bmatrix} 0 & 0 & 0 & 0 \\ 0 & 0 & 0 & 0 \\ 0 & 0 & 0 & 0 \\ C_{2i+2}^h & 0 & 0 & 0 \end{bmatrix},$$

(4.17c)

$$V_{i+1} = \begin{bmatrix} A_{i+2}^{2h} & -C_{i+2}^{2h} \\ -D_{i+3}^{2h} & A_{i+3}^{2h} \end{bmatrix}^{-1} \begin{bmatrix} S_{2i+3,1} & S_{2i+3,2} & 0 & 0 \\ 0 & 0 & S_{2i+5,1} & S_{2i+5,2} \end{bmatrix} \begin{bmatrix} 0 & 0 & 0 & D_{2i+3} \\ 0 & 0 & 0 & 0 \\ 0 & 0 & 0 & 0 \\ 0 & 0 & 0 & 0 \end{bmatrix},$$

where $A_k^{2h}, C_k^{2h}, D_k^{2h}$ are defined by (4.7), $S_{k,1}, S_{k,2}$ are defined by (4.5) and A_k^h, C_k^h, D_k^h are defined by (4.2).

Lemma 3 When $\max(\sigma_t h_{2i-1}, \sigma_t h_{2i}, \sigma_t h_{2i+1}, \sigma_t h_{2i+2}) \ll 1$, then,

$$(4.18a) \quad \|H_i\|_{1,\infty} \leq c_2 \frac{\max(\sigma_t(h_{2i-1} + h_{2i}), \sigma_t(h_{2i+1} + h_{2i+2}))}{\min(\sigma_t h_{2i-1}, \sigma_t h_{2i}, \sigma_t h_{2i+1}, \sigma_t h_{2i+2})},$$

$$(4.18b) \quad \|U_{i+1}\|_{1,\infty} \leq c_3 \frac{\max(\sigma_t(h_{2i-1} + h_{2i}), \sigma_t(h_{2i+1} + h_{2i+2}))}{\sigma_t(h_{2i+1} + h_{2i+2})},$$

$$(4.18c) \quad \|V_{i+1}\|_{1,\infty} \leq c_3 \frac{\max(\sigma_t(h_{2i+3} + h_{2i+4}), \sigma_t(h_{2i+5} + h_{2i+6}))}{\sigma_t(h_{2i+3} + h_{2i+4})},$$

where c_2 , and c_3 are constants independent of mesh sizes.

Proof: When $\max(\sigma_t h_{2i-1}, \sigma_t h_{2i}, \sigma_t h_{2i+1}, \sigma_t h_{2i+2}) \ll 1$, $\|B_k^h\| \ll 1, k = 2i-1, 2i, 2i+1, 2i+2$ in (4.2). By taking the dominant terms, we have

$$(4.19) \quad \begin{bmatrix} S_{2i-1,1} & S_{2i-1,2} & 0 & 0 \\ 0 & 0 & S_{2i,1} & S_{2i,2} \end{bmatrix} \begin{bmatrix} A_{2i-1}^h & -C_{2i-1}^h & 0 & 0 \\ -D_{2i}^h & A_{2i}^h & -C_{2i}^h & 0 \\ 0 & -D_{2i+1}^h & A_{2i+1}^h & -C_{2i+1}^h \\ 0 & 0 & -D_{2i+2}^h & A_{2i+2}^h \end{bmatrix} \\ = \begin{bmatrix} H_{11} & H_{12} & H_{13} & 0 \\ 0 & H_{22} & H_{23} & H_{24} \end{bmatrix} + O(1),$$

where

$$(4.20a) \quad H_{11} = \begin{bmatrix} \frac{2}{\sigma_t h_{2i-1}} M & 0 & -\frac{2}{\sigma_t h_{2i-1}} M & 0 \\ 0 & 0 & 0 & 0 \\ \frac{1}{\sigma_t(h_{2i-1}+h_{2i})} M & 0 & 0 & 0 \\ 0 & 0 & 0 & 0 \end{bmatrix},$$

$$(4.20b) \quad H_{12} = \begin{bmatrix} 0 & 0 & 0 & 0 \\ 0 & 0 & 0 & \frac{1}{\sigma_t(h_{2i-1}+h_{2i})} M \\ 0 & 0 & 0 & 0 \\ 0 & -\frac{2}{\sigma_t h_{2i}} M & 0 & \frac{2}{\sigma_t h_{2i}} M \end{bmatrix},$$

$$(4.20c) \quad H_{13} = \begin{bmatrix} 0 & 0 & 0 & 0 \\ 0 & 0 & 0 & 0 \\ -\frac{1}{\sigma_t(h_{2i-1}+h_{2i})}M & 0 & 0 & 0 \\ 0 & 0 & 0 & 0 \end{bmatrix},$$

$$(4.20d) \quad H_{22} = \begin{bmatrix} 0 & 0 & 0 & 0 \\ 0 & 0 & 0 & -\frac{1}{\sigma_t(h_{2i+1}+h_{2i+2})}M \\ 0 & 0 & 0 & 0 \\ 0 & 0 & 0 & 0 \end{bmatrix},$$

$$(4.20e) \quad H_{23} = \begin{bmatrix} \frac{2}{\sigma_t h_{2i+1}}M & 0 & -\frac{2}{\sigma_t h_{2i+1}}M & 0 \\ 0 & 0 & 0 & 0 \\ \frac{1}{\sigma_t(h_{2i+1}+h_{2i+2})}M & 0 & 0 & 0 \\ 0 & 0 & 0 & 0 \end{bmatrix},$$

$$(4.20f) \quad H_{24} = \begin{bmatrix} 0 & 0 & 0 & 0 \\ 0 & 0 & 0 & \frac{1}{\sigma_t(h_{2i+1}+h_{2i+2})}M \\ 0 & 0 & 0 & 0 \\ 0 & -\frac{2}{\sigma_t h_{2i+2}}M & 0 & \frac{2}{\sigma_t h_{2i+2}}M \end{bmatrix}.$$

Since M is constant, we can find a c_4 such that

$$(4.21) \quad \left\| \begin{bmatrix} S_{2i-1,1} & S_{2i-1,2} & 0 & 0 \\ 0 & 0 & S_{2i,1} & S_{2i,2} \end{bmatrix} \begin{bmatrix} A_{2i-1}^h & -C_{2i-1}^h & 0 & 0 \\ -D_{2i}^h & A_{2i}^h & -C_{2i}^h & 0 \\ 0 & -D_{2i+1}^h & A_{2i+1}^h & -C_{2i+1}^h \\ 0 & 0 & -D_{2i+2}^h & A_{2i+2}^h \end{bmatrix} \right\|_{1,\infty} \\ \leq \frac{c_4}{\min(\sigma_t h_{2i-1}, \sigma_t h_{2i}, \sigma_t h_{2i+1}, \sigma_t h_{2i+2})}.$$

Combined with *Lemma 2*, we have

$$(4.22) \quad \|H_i\|_{1,\infty} \leq c_2 \frac{\max(\sigma_t(h_{2i-1} + h_{2i}), \sigma_t(h_{2i+1} + h_{2i+2}))}{\min(\sigma_t h_{2i-1}, \sigma_t h_{2i}, \sigma_t h_{2i+1}, \sigma_t h_{2i+2})},$$

with $c_2 = c_1 c_4$.

To prove (4.18b), we have

$$(4.23) \quad \begin{bmatrix} S_{2i-1,1} & S_{2i-1,2} & 0 & 0 \\ 0 & 0 & S_{2i+1,1} & S_{2i+1,2} \end{bmatrix} \begin{bmatrix} 0 & 0 & 0 & 0 \\ 0 & 0 & 0 & 0 \\ 0 & 0 & 0 & 0 \\ C_{2i+2} & 0 & 0 & 0 \end{bmatrix} = \begin{bmatrix} 0 & 0 & 0 & 0 \\ U_{21} & 0 & 0 & 0 \end{bmatrix},$$

where c_8 is a constant independent of $\hat{\sigma}_t h_i$. \square

With all the lemmas established, we present in the next Theorem an upper bound on the convergence factor of multigrid algorithm when $\max_{k=(1,\dots,m)} (\sigma_t h_k) \ll 1$.

Theorem 5 *When $\max_{k=(1,\dots,m)} (\sigma_t h_k) \ll 1$ and (4.25) holds for all i , a two-grid multigrid $V(1,0)$ with two-cell red-black block μ -line relaxation will have a convergence factor which is less than $O(\max_{k=(1,\dots,m)} (\sigma_t^2 h_k^2))$.*

Proof: From Theorem 2, the errors after two-cell red-black block μ -line relaxation can be expressed as

$$(4.34) \quad \underline{e}_1^h = I_{2h}^h \underline{e}^{2h} + O(\max_{k=(1,\dots,m)} (\sigma_t^2 h_k^2)) \underline{e}_0^h.$$

A multigrid $V(1,0)$ cycle in matrix form takes the form of

$$(4.35) \quad \underline{e}_2^h = G^h \underline{e}_0^h - I_{2h}^h (A^{2h})^{-1} I_h^{2h} A^h G^h \underline{e}_0^h.$$

Substitute (4.34) into (4.35), we have

$$(4.36) \quad \begin{aligned} \underline{e}_2^h &= I_{2h}^h \underline{e}^{2h} + O(\max_{k=(1,\dots,m)} (\sigma_t^2 h_k^2)) \underline{e}_0^h - I_{2h}^h (A^{2h})^{-1} I_h^{2h} A^h I_{2h}^h \underline{e}^{2h} \\ &\quad + I_{2h}^h (A^{2h})^{-1} I_h^{2h} A^h O(\max_{k=(1,\dots,m)} (\sigma_t^2 h_k^2)) \underline{e}_0^h \\ &= O(\max_{k=(1,\dots,m)} (\sigma_t^2 h_k^2)) \underline{e}_0^h + I_{2h}^h (A^{2h})^{-1} I_h^{2h} A^h O(\max_{k=(1,\dots,m)} (\sigma_t^2 h_k^2)) \underline{e}_0^h. \end{aligned}$$

Note that

$$(4.37) \quad I_{2h}^h \underline{e}^{2h} = I_{2h}^h (A^{2h})^{-1} I_h^{2h} A^h I_{2h}^h \underline{e}^{2h}.$$

It is obvious that we only need to bound the norm of $I_{2h}^h (A^{2h})^{-1} I_h^{2h} A^h$.

From (4.29), we obtain

$$(4.38) \quad (A^{2h})^{-1} I_h^{2h} A^h = (I - Z_1^{-1} Z_2)^{-1} Z_1^{-1} I_h^{2h} A^h,$$

and

$$(4.39) \quad Z_1^{-1} I_h^{2h} A^h = \begin{bmatrix} H_1 & -U_2 & & & \\ -V_2 & H_3 & & & \\ & & \ddots & & \\ & & & -V_{m-2} & H_{m-1} \end{bmatrix}.$$

By our assumption of (4.25) and (4.26), we have

$$(4.40) \quad \|Z_1^{-1}I_h^{2h}A^h\|_{1,\infty} \leq c_9.$$

For any matrix A , $\|A\|_2 \leq \sqrt{\|A\|_1\|A\|_\infty}$. So

$$(4.41) \quad \|Z_1^{-1}I_h^{2h}A^h\|_2 \leq c_9.$$

The norms of I_{2h}^h are bounded by a constant. So

$$(4.42) \quad \|I_{2h}^h\|_2 < c_{10}.$$

Combining *Lemma 4* with Equations (4.41) and (4.42), we obtain

$$(4.43) \quad \|\underline{\mathcal{E}}_2^h\|_2 / \|\underline{\mathcal{E}}_0^h\|_2 < O\left(\max_{k=(1,\dots,m)} (\sigma_t^2 h_k^2)\right).$$

□

When $\min_{k=(1,\dots,m)} (\sigma_t h_k) \gg 1$, we limit our analysis to only four cells on the fine grid with uniform mesh size h and our numerical results imply that the analytical result is valid with nonuniform mesh size and large number of cells. The next theorem gives an upper bound on convergence factor of multigrid algorithm when $m = 4$ and $\sigma_t h \gg 1$. First, let us establish some space saving notation. Define the block matrices

$$(4.44) \quad E_{j,l} = [0, \dots, 0, I, 0, \dots, 0],$$

to have l blocks of size $n \times n$ with the I appearing as the j th block. Then we define another block matrix with $n \times n$ blocks, say

$$(4.45) \quad W = [W_1, \dots, W_k].$$

The product $W^T E_{j,l}$ is a $k \times l$ block matrix with $n \times n$ blocks. Each block column is zero except the j th block column which contains W^T . For example, we may write C_i in (2.18b) as

$$(4.46) \quad C_i = \begin{bmatrix} 0 & 0 & 0 & 0 \\ 0 & 0 & 0 & 0 \\ B_i & 0 & 0 & 0 \\ 0 & 0 & 0 & 0 \end{bmatrix} = [0, 0, B_i, 0]^T E_{1,4}.$$

Theorem 6: When there are four uniform cells on the fine grid and $\sigma_t h \gg 1$, a multigrid $V(1,1)$ cycle with two-cell red-black block μ -line relaxation will have a convergence factor $\rho \leq c(\frac{1}{\sigma_t h})$ for some c independent of $\sigma_t h$.

Proof: Define A^h as the fine grid operator, then

$$(4.47) \quad A^h = \begin{bmatrix} A & -C \\ -D & A \end{bmatrix},$$

where

$$(4.48a) \quad A = \begin{bmatrix} I + 2B - R & -2R & -2B & R & 0 & 0 & 0 & 0 \\ 0 & I - R & -R & B & 0 & 0 & 0 & 0 \\ B & -R & I - R & 0 & -B & 0 & 0 & 0 \\ R & -2B & -2R & I + 2B - R & 0 & 0 & 0 & 0 \\ 0 & 0 & 0 & 0 & I + 2B - R & -2R & -2B & R \\ 0 & 0 & 0 & -B & 0 & I - R & -R & B \\ 0 & 0 & 0 & 0 & B & -R & I - R & 0 \\ 0 & 0 & 0 & 0 & R & -2B & -2R & I + 2B - R \end{bmatrix},$$

and

$$(4.48b) \quad C = \begin{bmatrix} 0 & 0 & 0 & 0 & 0 & 0 & B & 0 \end{bmatrix}^T E_{1,8}, \quad D = \begin{bmatrix} 0 & B & 0 & 0 & 0 & 0 & 0 & 0 \end{bmatrix}^T E_{8,8}.$$

The coarse grid operator A^{2h} is defined by

$$(4.49) \quad A^{2h} = I_h^{2h} A^h I_{2h}^h,$$

with I_h^{2h} and I_{2h}^h defined by

$$(4.50a) \quad I_h^{2h} = \begin{bmatrix} S_1 & S_2 & 0 & 0 \\ 0 & 0 & S_1 & S_2 \end{bmatrix}, \quad S_1 = \begin{bmatrix} I & 0 & 0 & 0 \\ 0 & 0.5I & 0 & 0 \\ 0 & 0 & 0.5I & 0 \\ 0 & 0 & 0 & 0 \end{bmatrix}, \quad S_2 = \begin{bmatrix} 0 & 0 & 0 & 0 \\ 0 & 0.5I & 0 & 0 \\ 0 & 0 & 0.5I & 0 \\ 0 & 0 & 0 & I \end{bmatrix},$$

$$(4.50b) \quad I_{2h}^h = \begin{bmatrix} T_1 & 0 \\ T_2 & 0 \\ 0 & T_1 \\ 0 & T_2 \end{bmatrix}, \quad T_1 = \begin{bmatrix} I & 0 & 0 & 0 \\ 0 & 1.5I & 0 & -0.5I \\ 0.5I & 0 & 0.5I & 0 \\ 0 & I & 0 & 0 \end{bmatrix}, \quad T_2 = \begin{bmatrix} 0 & 0 & I & 0 \\ 0 & 0.5I & 0 & 0.5I \\ -0.5I & 0 & 1.5I & 0 \\ 0 & 0 & 0 & I \end{bmatrix}.$$

The red-black relaxation matrix G^h is

$$(4.51) \quad G^h = \begin{bmatrix} A & 0 \\ -D & A \end{bmatrix}^{-1} \begin{bmatrix} 0 & C \\ 0 & 0 \end{bmatrix} = \begin{bmatrix} 0 & A^{-1}C \\ 0 & A^{-1}DA^{-1}C \end{bmatrix}.$$

A $V(1, 1)$ multigrid cycle can be written in matrix form as

$$(4.52) \quad \underline{e}_2^h = G^h(G^h - I_{2h}^h(A^{2h})^{-1}I_h^{2h}A^hG^h)\underline{e}_0^h,$$

here \underline{e}_0^h is the initial error and \underline{e}_2^h is the error after the $V(1, 1)$ cycle.

Multiply G^h by A^h on the left to get

$$(4.53) \quad A^h G^h = \begin{bmatrix} 0 & C - CA^{-1}DA^{-1}C \\ 0 & 0 \end{bmatrix} = \begin{bmatrix} C & 0 \\ 0 & 0 \end{bmatrix} \begin{bmatrix} 0 & I - A^{-1}DA^{-1}C \\ 0 & 0 \end{bmatrix}.$$

Note that

$$(4.54) \quad I_h^{2h} \begin{bmatrix} C & 0 \\ 0 & 0 \end{bmatrix} = \begin{bmatrix} 0 & 0 & \frac{1}{2}B & 0 & 0 & 0 & 0 & 0 & 0 \end{bmatrix}^T E_{1,16}.$$

The expansion of $(A^{2h})^{-1}I_h^{2h} \begin{bmatrix} C & 0 \\ 0 & 0 \end{bmatrix}$ is

$$(4.55) \quad (A^{2h})^{-1}I_h^{2h} \begin{bmatrix} C & 0 \\ 0 & 0 \end{bmatrix} = \frac{\sigma_i h}{4c_2} \begin{bmatrix} 0 \\ RM \\ RM \\ 2RM \\ 2RM \\ RM \\ RM \\ 0 \end{bmatrix} E_{1,16}$$

$$+ \frac{1}{2c_1} \begin{bmatrix} \frac{1}{2}RM + \frac{c_1}{2c_2}MRM \\ \frac{1}{8}(3 + \frac{3c_1c_3}{c_2^2})RM - \frac{c_1}{2c_2}MRM - \frac{c_1}{4c_2}RM^2 \\ \frac{1}{8}(3 + \frac{3c_1c_3}{c_2^2})RM + \frac{c_1}{2c_2}MRM - \frac{c_1}{4c_2}RM^2 \\ \frac{1}{4}(3 + \frac{3c_1c_3}{c_2^2})RM - \frac{c_1}{2c_2}MRM - \frac{c_1}{2c_2}RM^2 \\ \frac{1}{4}(-1 + \frac{3c_1c_3}{c_2^2})RM - \frac{c_1}{2c_2}MRM - \frac{c_1}{2c_2}RM^2 \\ \frac{1}{8}(1 + \frac{3c_1c_3}{c_2^2})RM + \frac{c_1}{2c_2}MRM - \frac{c_1}{4c_2}RM^2 \\ \frac{1}{8}(1 + \frac{3c_1c_3}{c_2^2})RM - \frac{c_1}{4c_2}MRM - \frac{c_1}{4c_2}RM^2 \\ \frac{1}{2}RM + \frac{c_1}{2c_2}MRM \end{bmatrix} E_{1,16} + O(\frac{1}{\sigma_i h}),$$

where $M = \sigma_i h B$ and $c_1 = \sum_{j=1}^n \omega_j \mu_j$, $c_2 = \sum_{j=1}^n \omega_j \mu_j^2$ and $c_3 = \sum_{j=1}^n \omega_j \mu_j^3$. Note $RM R = c_1 R$, $RM^2 R = c_2 R$ and $RM^3 R = c_3 R$.

Expand $I - A^{-1}DA^{-1}C$ as

$$(4.56) \quad I - A^{-1}DA^{-1}C = I - \frac{1}{4c_1} \begin{bmatrix} 4RM \\ 3RM \\ 3RM \\ 2RM \\ 2RM \\ RM \\ RM \\ 0 \end{bmatrix} E_{1,8}.$$

$$-\frac{1}{8c_1^2\sigma_t h} \begin{bmatrix} -8c_2RM - 4c_1MRM - 4c_1RM^2 \\ -5c_2RM + 4c_1MRM - \frac{1}{4}(13 - \frac{c_1c_3}{c_2^2})c_1RM^2 \\ -5c_2RM - 4c_1MRM - \frac{1}{4}(13 - \frac{c_1c_3}{c_2^2})c_1RM^2 \\ -2c_2RM + 4c_1MRM - \frac{1}{2}(5 - \frac{c_1c_3}{c_2^2})c_1RM^2 \\ -2c_2RM - 4c_1MRM - \frac{1}{2}(5 - \frac{c_1c_3}{c_2^2})c_1RM^2 \\ c_2RM - 4c_1MRM - \frac{1}{4}(5 - \frac{c_1c_3}{c_2^2})c_1RM^2 \\ c_2RM + 4c_1MRM - \frac{1}{4}(5 - \frac{c_1c_3}{c_2^2})c_1RM^2 \\ 4c_2RM + 4c_1MRM \end{bmatrix} E_{1,8} + O(\frac{1}{\sigma_t^2 h^2})$$

From (4.55) and (4.56), we get

$$(4.57) \quad (A^{2h})^{-1}I_h^{2h} \begin{bmatrix} C & 0 \\ 0 & 0 \end{bmatrix} \begin{bmatrix} 0 & I - A^{-1}DA^{-1}C \\ 0 & 0 \end{bmatrix} = \frac{1}{4c_1} \begin{bmatrix} 0 \\ 2RM \\ 2RM \\ 4RM \\ 4RM \\ 2RM \\ 2RM \\ 0 \end{bmatrix} E_{9,16} + O(\frac{1}{\sigma_t h}).$$

Then

$$(4.58) \quad I_{2h}^h (A^{2h})^{-1} I_h^{2h} A^h G^h = \frac{1}{4c_1} \begin{bmatrix} 0 \\ RM \\ RM \\ 2RM \\ 2RM \\ 3RM \\ 3RM \\ 4RM \\ 4RM \\ 3RM \\ 3RM \\ 2RM \\ 2RM \\ RM \\ RM \\ 0 \end{bmatrix} E_{9,16} + O(\frac{1}{\sigma_t h}).$$

The expansion of G^h takes the form of

$$(4.59) \quad G^h = \frac{1}{4c_1} \begin{bmatrix} 0 \\ \frac{1}{2}RM + \frac{c_1}{2c_2}RM^2 \\ \frac{1}{2}RM + \frac{c_1}{2c_2}RM^2 \\ RM + \frac{c_1}{c_2}RM^2 \\ RM + \frac{c_1}{c_2}RM^2 \\ \frac{5}{2}RM + \frac{c_1}{2c_2}RM^2 \\ \frac{5}{2}RM + \frac{c_1}{2c_2}RM^2 \\ 4RM \\ 4RM \\ 3RM \\ 3RM \\ 2RM \\ 2RM \\ RM \\ RM \\ 0 \end{bmatrix} E_{9,16} + O\left(\frac{1}{\sigma_i h}\right).$$

So

$$(4.60) \quad G^h G^h = \frac{1}{4c_1} \begin{bmatrix} 0 \\ RM \\ RM \\ 2RM \\ 2RM \\ 3RM \\ 3RM \\ 4RM \\ 4RM \\ 3RM \\ 3RM \\ 2RM \\ 2RM \\ RM \\ RM \\ 0 \end{bmatrix} E_{9,16} + O\left(\frac{1}{\sigma_i h}\right)$$

and

$$(4.61) \quad G^h I_{2h}^h (A^{2h})^{-1} I_h^{2h} A^h G^h = \frac{1}{4c_1} \begin{bmatrix} 0 \\ RM \\ RM \\ 2RM \\ 2RM \\ 3RM \\ 3RM \\ 4RM \\ 4RM \\ 3RM \\ 3RM \\ 2RM \\ 2RM \\ RM \\ RM \\ 0 \end{bmatrix} E_{9,16} + O\left(\frac{1}{\sigma_t h}\right).$$

Combine (4.60) and (4.61), we can have

$$(4.62) \quad \|G^h(G^h - I_{2h}^h(A^{2h})^{-1}I_h^{2h}A^hG^h)\| \leq \frac{c}{\sigma_t h}.$$

here c is a constant independent of $\sigma_t h$. \square

§5 Computational Results

5.1 Multigrid Convergence Rates

The following computational results were conducted on a computational domain with $m = 1024$ and S_8 , that is $n = 4$. Our analytical results are independent of n . From the computational results conducted on S_N with N ranging from 2 to 256, we observe a convergence performance independent of N .

1. Convergence Factor for Uniform Grid

The results in Table 1 reveal that the convergence factor ρ is $O(\sigma_t^3 h^3)$ when $\sigma_t h \ll 1$ and is $O(\frac{1}{\sigma_t^2 h^2})$ when $\sigma_t h \gg 1$. The computational results are even better than the analytical results. Our analysis only gives upper bounds on the convergence factor. We believe that the numerical results reflect the actual behavior. In Table 2, we present a range within which the maximal convergence factor occurs. Note that the maximal ρ occurs around $\sigma_t h = 0.01$.

$\sigma_t h$	convergence factor ρ
10^{-6}	0.23×10^{-10}
10^{-5}	0.21×10^{-7}
10^{-4}	0.16×10^{-4}
10^{-3}	0.20×10^{-2}
10^{-2}	0.97×10^{-2}
10^{-1}	0.89×10^{-2}
1	0.58×10^{-3}
10^1	0.27×10^{-4}
10^2	0.20×10^{-6}
10^3	0.20×10^{-8}
10^4	0.20×10^{-10}

Table 1. Convergence Factors for Uniform Grid

$\sigma_t h$	convergence factor ρ
0.005	0.72×10^{-2}
0.006	0.87×10^{-2}
0.007	0.95×10^{-2}
0.008	0.98×10^{-2}
0.009	0.98×10^{-2}
0.010	0.97×10^{-2}
0.011	0.96×10^{-2}
0.012	0.96×10^{-2}
0.013	0.95×10^{-2}
0.014	0.95×10^{-2}
0.015	0.95×10^{-2}

Table 2. Convergence Factors for Uniform Grid: Worst Case

2. Convergence Factor for Nonuniform Grid

We choose a highly variable $\sigma_t h_i$ by letting $\sigma_t h_i = c10^{2\eta_i}$, $i = 1, \dots, m$ where η_i is a random number between $(-1, 1)$. Thus, neighboring cells can vary in width up to 4 orders of magnitude. Here, c is a constant chosen to control the range of cell widths. If $c = 1$, then $\sigma_t h_i$ are random numbers between $(0.01, 100)$. If $c \geq 100$, $\sigma_t h_i \geq 1$. If $c \leq 0.01$, all $\sigma_t h_i \leq 1$. The results of Table 3 indicate that the performance of our multigrid scheme for a nonuniform grid is the same as for a uniform grid. Furthermore in both thin and thick limit cases, a nonuniform grid has the same convergence behavior as uniform grid.

c	convergence factor ρ
1.0^{-6}	9.9×10^{-10}
1.0^{-5}	8.5×10^{-7}
1.0^{-4}	2.7×10^{-4}
1.0^{-3}	5.4×10^{-3}
1.0	9.1×10^{-4}
1.0^2	3.3×10^{-4}
1.0^3	6.1×10^{-6}
1.0^4	2.4×10^{-8}
1.0^5	2.3×10^{-10}

Table 3. Convergence Factors for Nonuniform Grids

5.2 DSA Convergence Rates

As was mentioned in the introduction, a competing algorithm for the solution of the isotropic S_N equations in slab geometry is Diffusion Synthetic Acceleration (DSA). It is motivated by the observation that, in the thick limit, the solution of the linear Boltzman equation (1.1) becomes independent of angle except near boundaries and sources. If the S_N problem were recast as an S_2 problem, then the zeroth and first Legendre moments of the solution could be found by solving a diffusion equation for the zeroth moment. DSA can be viewed as a preconditioning technique (Faber and Manteuffel [5]) or as a two level multigrid scheme (Larson [7]) in which an S_2 problem is used as a coarse level correction to an S_N problem. In this context, a transport sweep or x -line relaxation (see(3.3)) corresponds to multigrid relaxation and the S_2 problem represents the coarse level. DSA skips all of the intermediate levels. The multigrid in angle scheme developed in Morel and Manteuffel [15] visits levels $N, N/2, N/4, \dots, 2$ and is effective for isotropic scattering as well as highly anisotropic scattering.

The overall DSA algorithm is very sensitive to the difference scheme used to solve the diffusion equation. In our numerical results we solve an S_2 equation discretized with a MLD scheme using Marshak boundary conditions as the coarse level correction. This is equivalent to solving a consistently differenced diffusion equation for the zeroth moment. In Table 4 and Table 5 we present convergence factors for a $V(1, 1)$ multigrid cycle and for a DSA cycle. Here, the slab is assumed to have physical thickness 1. Thus, σ_t represents the width of the slab measured in the number of mean-free-paths. The tests were performed using S_8 and a wide range of σ_t and m , (the number of cells). The diagonals of these tables represent constant $\sigma_t h$.

σ_t	$m = 16$	$m = 64$	$m = 256$	$m = 1024$	$m = 4096$
4^{-5}	.12E-9	.16E-9	.16E-9	.16E-9	.16E-9
4^{-4}	.72E-8	.10E-7	.10E-7	.10E-7	.10E-7
4^{-3}	.37E-6	.55E-6	.56E-6	.56E-6	.56E-6
4^{-2}	.17E-4	.16E-4	.18E-4	.26E-4	.27E-4
4^{-1}	.25E-3	.53E-3	.55E-3	.55E-4	.58E-4
1	.14E-2	.37E-2	.44E-2	.44E-2	.46E-2
4	.82E-3	.35E-2	.82E-2	.99E-2	.99E-2
16	.57E-3	.13E-2	.63E-2	.86E-2	.97E-2
64	.46E-4	.57E-3	.23E-2	.85E-2	.99E-2
256	.20E-5	.46E-4	.58E-3	.25E-2	.89E-2
1024	.12E-6	.18E-5	.47E-4	.58E-3	.26E-2
4096	.75E-8	.12E-6	.16E-5	.46E-4	.58E-3
8192	.45E-9	.75E-8	.12E-6	.14E-5	.47E-4
16384	.28E-10	.46E-9	.75E-8	.12E-6	.11E-5
32768	.18E-11	.30E-10	.47E-9	.75E-8	.12E-6
65536	.11E-12	.20E-11	.30E-10	.46E-9	.75E-8

Table 4. Convergence Factors for the Multigrid Algorithm

σ_t	$m = 16$	$m = 64$	$m = 256$	$m = 1024$	$m = 4096$
4^{-5}	.190E-2	.190E-2	.190E-2	.190E-2	.190E-2
4^{-4}	.747E-2	.746E-2	.746E-2	.747E-2	.747E-2
4^{-3}	.276E-1	.276E-1	.276E-1	.276E-1	.276E-1
4^{-2}	.836E-1	.834E-1	.834E-1	.835E-1	.835E-1
4^{-1}	.153	.151	.151	.152	.152
1	.188	.203	.204	.204	.205
4	.180	.217	.216	.217	.218
16	.142	.164	.204	.217	.219
64	.129	.143	.149	.165	.185
256	.125	.131	.143	.145	.160
1024	.124	.126	.131	.143	.146
4096	.124	.124	.126	.131	.142
8192	.124	.124	.126	.127	.132
16384	.124	.124	.124	.126	.126
32768	.124	.124	.124	.124	.126
65536	.124	.124	.124	.124	.124

Table 5. Convergence Factors for the DSA Algorithm

For the multigrid algorithm, the convergence factors are roughly equal along diagonals, with the slowest rates occurring for $\sigma_t h$ in the range 4^{-3} (.0156) to 4^{-5} (.97E-3). For example, $\sigma_t = 4^{-1}$, $m = 16$ and $\sigma_t = 64$, $m = 4096$ are on the diagonal with $\sigma_t h = .0156$.

The behavior of the DSA algorithm is quite different. The best rate achieved for thick problems is .124. Further, for any fixed $\sigma_t \geq 4$, the slab is thick but the cells become individually thin as the number of cells increases. In this limit DSA saturates to a convergence factor of .23. In our tests the value of m was not quite large enough to achieve this limit, but a value of .219 was reached for $\sigma_t = 16$ and $m = 4096$.

In all cases, the multigrid convergence factors were superior to the DSA convergence factors. However, it is important to adjust for the relative amount of computational work required by each algorithm. Of course, such measures will be machine dependent. On the Cray Y/MP, where these tests were performed, we compared times for $N=64$ and $m=1024$. The V(1,1) cycle required 8.9 seconds and the DSA cycle required 3.7 seconds. The ratio of these times is 2.4. Table 6 is the result of raising each term in Table 5 to the power 2.4. This is a more fair comparison with Table 4 on a serial machine. Note that the multigrid algorithm is faster than DSA in all regimes. On a parallel machine we expect the results to more heavily favor the multigrid algorithm. Both algorithms can be implemented with parallel complexity $O(\log(m))$. In this context, however, we expect the times required to perform a single DSA cycle and a single multigrid V(1,1) cycle to be more nearly equal. A parallel version of the multigrid algorithm is described in [10], [11]. A parallel version of the DSA sweep has also been implemented on the Thinking Machines Inc. CM-200 at Los Alamos National Laboratories [20].

σ_t	$m = 16$	$m = 64$	$m = 256$	$m = 1024$	$m = 4096$
4^{-5}	.29E-6	.29E-6	.29E-6	.29E-6	.29E-6
4^{-4}	.78E-5	.78E-5	.78E-5	.78E-5	.78E-5
4^{-3}	.18E-3	.18E-3	.18E-3	.18E-3	.18E-3
4^{-2}	.25E-2	.25E-2	.25E-2	.25E-2	.25E-2
4^{-1}	.11E-1	.10E-1	.10E-1	.10E-1	.10E-1
1	.18E-1	.21E-1	.22E-1	.22E-1	.22E-1
4	.16E-1	.25E-1	.25E-1	.25E-1	.25E-1
16	.92E-2	.13E-1	.22E-1	.25E-1	.26E-1
64	.73E-2	.93E-2	.10E-1	.13E-1	.17E-1
256	.68E-2	.76E-2	.93E-2	.97E-2	.12E-1
1024	.66E-2	.69E-2	.76E-2	.93E-2	.98E-2
4096	.66E-2	.66E-2	.69E-2	.76E-2	.92E-2
8192	.66E-2	.66E-2	.69E-2	.70E-2	.77E-2
16384	.66E-2	.66E-2	.66E-2	.69E-2	.69E-2
32768	.66E-2	.66E-2	.66E-2	.66E-2	.69E-2
65536	.66E-2	.66E-2	.66E-2	.66E-2	.66E-2

Table 6. Adjusted Convergence Factors for the DSA Algorithm

In either setting, parallel or serial, a full multigrid algorithm can be implemented (cf.[13]). This version of multigrid starts on a coarse grid and moves toward finer grids. In general, an amount of work equal to two V(1,1) cycles on the finest grid will yield a solution that is accurate to the level of discretization error. This would provide a savings in some regions of the tables. Moreover, full multigrid provides a natural framework for adaptive grid refinement.

§6 Conclusions

From our numerical and analytical results, we conclude that

- For S_2 , two-cell, red-black, block μ -line relaxation is a good smoother which makes the errors exactly in the range of interpolation after one relaxation. Thus, one multigrid V(1,0) cycle is an exact solver for the S_2 problem.
- For S_N with $N > 2$, the errors at two neighboring cells $2i - 1$, $2i$ after one such relaxation will be in the range of interpolation up to accuracy of $O(\max(\frac{1}{\sigma_t h_{2i-1}}, \frac{1}{\sigma_t h_{2i}}))$ when $\min(\sigma_t h_{2i-1}, \sigma_t h_{2i}) \gg 1$ and $O(\max(\sigma_t^2 h_{2i-1}^2, \sigma_t^2 h_{2i}^2))$ when $\max(\sigma_t h_{2i-1}, \sigma_t h_{2i}) \ll 1$.
- The multigrid algorithm is an efficient solver which has a convergence factor of $O(\max_{k=(1,\dots,m)}(\frac{1}{\sigma_t^2 h_k^2}))$ for the thick limit and $O(\max_{k=(1,\dots,m)}(\sigma_t^3 h_k^3))$ for the thin limit with a maximal of $\rho = 0.0098$ occurring around $\sigma_t h = 0.01$ for the uniform grid.
- The multigrid algorithm performs equally well for uniform and nonuniform grids.
- In the thick limit a single V(1,1) yields nearly an exact solution.
- The multigrid algorithm is more efficient than DSA in all regimes.
- The relaxation is implemented in a red-black ordering and is parallelizable.

The above results assumed no absorption. The problem is easy to solve if the absorption is sufficiently large, that is if $\gamma = \frac{\sigma_s}{\sigma_t}$ is bounded away from unity. In this case, smoothing alone is sufficient for a fast solution. With no absorption, $\gamma = 1$, the algorithm presented above provides nearly an exact solver. However, for the case in which $\gamma = 1 - O(\frac{1}{(\sigma_t h)^2})$ in the thick limit, the above algorithm yields a convergence factor that does not go to zero in the thick limit. A minor adaptation to the algorithm has been developed that treats this special case and provides a convergence factor that does go to zero in the thick limit for all levels of absorption. It will appear in a subsequent report.

References

- [1] M. L. Adams and W. R. Martin, "Diffusion-Synthetic Acceleration of Discontinuous Finite-Element Transport Iterations," *Nucl. Sci. Eng.*, **111**, 145-167 (1992).

- [2] R. E. Alcouffe, "Diffusion Synthetic Acceleration Methods for the Diamond-Differenced Discrete-Ordinates Equations," *Nucl. Sci. Eng.*, **64**, 344 (1977).
- [3] Allen Barnett, J. E. Morel, and D. R. Harris, "A Multigrid Acceleration Method for the One-Dimensional S_n Equations with Anisotropic Scattering," *Nucl. Sci. Eng.*, **102**, 1 (1989).
- [4] A. Brandt, Multi-level Adaptive Solution to Boundary-value Problems. *Math. Comp.*, **31**, 333 (1977).
- [5] V. Faber and T. A. Manteuffel, "Neutron Transport from the Viewpoint of Linear Algebra Integral," *Transport Theory, Invariant Imbedding and Equations*, (Nelson, Faber, Manteuffel, Seth and White, eds.), Lecture Notes in Pure and Applied Mathematics, **115**, pp. 37-61, Marcel-Dekker, April, 1989.
- [6] E. W. Larsen, "Unconditionally Stable Diffusion-Synthetic Acceleration Methods for the Slab Geometry Discrete Ordinates Equations," *Nucl. Sci. Eng.*, **82**, 47 (1982).
- [7] E. W. Larsen, "Transport Acceleration Methods as Two-Level Multigrid Algorithms," *Operator Theory: Advances and Applications*, Vol. 51, p34-47, (1991).
- [8] E.W.Larsen, J.E. Morel, "Asymptotic Solutions of Numerical Transport Problems in Optically Thick Diffusive Regimes II," *J. Comp. Phys.*, **83**, 212 (1989).
- [9] E. E. Lewis and W. F. Miller, Jr., *Computational Methods of Neutron Transport*, John Wiley and Sons, (1984).
- [10] T. A. Manteuffel, S. F. McCormick, J. E. Morel, S. Oliveira, and G. Yang, "Parallel Multigrid Methods for Transport Equations," *Proceedings of the Copper Mountain Conference on Iterative Methods, Copper Mountain, CO, April 9 - 14, 1992*
- [11] T. A. Manteuffel, S. F. McCormick, J. E. Morel, S. Oliveira, and G. Yang, "A Parallel Version of a Multigrid Algorithm for Isotropic Transport Equations," *SIAM J. Sci Stat. Comp.*, Vol. 15, No. 2, (1994)
- [12] T. A. Manteuffel, S.F. McCormick, J. E. Morel and G. Yang, "A Fast Multigrid Algorithm for Transport Problems II: With Absorption," submitted to *SIAM J. Sci. and Stat. Comp.*, March, 1993.
- [13] S. F. McCormick, *Multilevel Adaptive Methods for Partial Differential Equations*, SIAM Press, (1989).
- [14] J. E. Morel and E. W. Larsen, "A Multiple Balance Approach for Differencing the S_N Equations," *Nucl. Sci. Eng.*, **105**, 1 (1990).
- [15] J. E. Morel and T. A. Manteuffel: "An Angular Multigrid Acceleration Technique for the S_N Equations With Highly Forward-Peaked Scattering," *Nucl. Sci. Eng.*, **107** 330 (1991).

- [16] P. F. Nowak, " A Coupled Synthetic and Multigrid Acceleration Method for Two-Dimensional Transport Calculations PhD thesis, Department of Nuclear Engineering, University of Michigan, 1988.
- [17] P. F. Nowak, *A Multigrid Method for S_N Calculations in x - y Geometry*, Transactions of the American Nuclear Society, vol. 56 pp. 291-292, 1988.
- [18] P. F. Nowak, E. W. Larsen, *Multigrid methods for S_N problems*, Transactions of the American Nuclear Society, vol. 57, pp. 355-356, 1987.
- [19] A. Nowak, J. E. Morel and D.R.Harris, *A Multigrid Acceleration Method for one dimensional S_N Equations with Anisotropic Scattering*, Nucl. Sci. Eng., 102,1 1989
- [20] S. Oliveira, "Parallel Multigrid Methods for Transport Equations ", Ph. D. Thesis, Department of Mathematics, University of Colorado at Denver, Denver, Co., May, 1993.